# Nano-engineered VEGF-C ameliorates gut lymphatic drainage, portal pressure and ascites in experimental portal hypertension

Savneet Kaur[1*#], Dinesh M Tripathi[1*], Pinky Juneja, Impreet Kaur[1], Sumati Rohilla[1], Abhishak Gupta[1], Preety Rawal[1], Angeera Yadav[4], Archana Rastogi[2], SM Shastry[3], V Rajan[3], VGM Naidu[4], Syed Nazrin Ruhina Rahman[5], Subham Banerjee[5#], Shiv K Sarin[3#].

**[1]Department of Molecular and Cellular Medicine, Institute of Liver and Biliary Sciences, New Delhi**

**[2]Department of Pathology, Institute of Liver and Biliary Sciences, New Delhi**

**[3]Department of Hepatology, Institute of Liver and Biliary Sciences, New Delhi**

**[4]Department of Pharmacology and Toxicology, National Institute of Pharmaceutical Education and Research (NIPER)-Guwahati, Changsari-781101, Assam, India.**

**[5]Department of Pharmaceutics, NIPER-Guwahati, Changsari-781101, Assam, India.**

*Shared first author

[#]Corresponding author

**[#]Correspondence**

Dr. Savneet Kaur, Assistant Professor, Department of Molecular and Cellular Medicine, Institute of Liver and Biliary Sciences, New Delhi, India, Phone no. 91-11-46300000, Email: savykaur@gmail.com

Prof. Shiv K Sarin, Director and Professor, Department of Hepatology, Institute of Liver and Biliary Sciences, New Delhi, India, Phone no. 91-11-46300000, Email: shivsarin@gmail.com

Dr. Subham Banerjee, Assistant Professor, Department of Pharmaceutics, NIPER-Guwahati, Changsari-781101, Assam, India, Email: banerjee.subham@yahoo.co.in

**Financial Support**

The study was funded by Department of Science and Technology (DST), Ministry of Science & Technology, Government of India (DST/NM/NT/2019/191).

## Abstract

**Objective:** Gut lymphatic vessels are crucial in maintaining abdominal fluid homeostasis. We studied these vessels in clinical cirrhosis and explored effects of vascular endothelial growth factor-C (VEGF-C), a pro-lymphangiogenic factor, in experimental portal hypertension. **Design:** Vascular endothelial growth factor receptor 3 (vegfr3)-positive lymphatic channels were enumerated in duodenal (D2) biopsies from cirrhotic patients. Vegfr3 antibody-tagged lipid nanocarriers were used to formulate novel nano-engineered (E-VEGF-C) molecule for targeted lymphangiogenesis of gut lymphatic vessels. The uptake of E-VEGF-C was evaluated in lymphatic endothelial cells (LyECs) *in vitro* and *in vivo*. The effects of E-VEGF-C were tested in cirrhotic and non-cirrhotic animal models of portal hypertension. Animals given nanocarriers alone served as vehicle. Mesenteric lymphatic vessel numbers/proliferation and drainage were analyzed. Abdominal ascites, hepatic and systemic hemodynamics was measured. Liver, duodenum, mesentery and plasma were examined. **Results:** In D2 biopsies, number of dilated vegfr3+ lymphatic vessels was significantly increased in decompensated as compared to compensated cirrhosis and correlated with presence of ascites. E-VEGF-C was efficiently taken up by the mesenteric LyECs. E-VEGF-C treated rats displayed a marked increase in the proliferation of mesenteric lymphatic vessels and drainage as compared to CCl4-vehicle. Ascites and mesenteric inflammation were markedly reduced in E-VEGF-C treated cirrhotic rats. Portal pressures were attenuated in both cirrhotic and non-cirrhotic portal hypertensive rats treated with E-VEGF-C as compared to respective vehicle groups. **Conclusion:** E-VEGF-C molecule enhances mesenteric lymphangiogenesis and improves lymphatic vessel drainage, attenuating abdominal

ascites and portal pressures. Targeted gut lymphangiogenesis may serve as an emerging therapy for portal hypertension.

**Significance of the Study**

What is already known about this subject?

- Gut lymphatic vessels play crucial roles in maintaining fluid and immune homeostasis in the abdomen.
- An increased but dysfunctional gut lymphangiogenesis occurs to compensate for lymphatic insufficiency in patients with gut inflammatory diseases.
- Therapies aimed at enhancing lymphangiogenesis with growth factors such as VEGF-C constitute an effective strategy to improve lymphatic drainage and ameliorate inflammation in certain pathologies.
- Gut lymphatic vessels remain poorly characterized in patients with cirrhosis.

What are the new findings?

- Dilated vegfr3+ lymphatic vessels are significantly increased in patients with decompensated as compared to compensated cirrhosis and correlated with presence of ascites.
- A nanoengineered pro-angiogenic molecule, E-VEGF-C with specificity for uptake by the gut lymphatic endothelial cells molecule enhances mesenteric lymphangiogenesis.
- E-VEGF-C improved lymphatic vessel drainage, attenuating abdominal ascites and portal pressures.

How might it impact on clinical practice in the foreseeable future?

- Gut lymphangiogenesis is proposed as an innovative strategy for the management of ascites and portal hypertension.

## Introduction

Chronic liver diseases cause significant morbidity and mortality worldwide. They can progress from mild fibrosis to portal hypertension to cirrhosis, which may further proceed to end-stage liver disease with onset of decompensation (e.g. ascites) and finally development of hepatocellular carcinoma (HCC). Along-side other underlying factors, a deranged gut-liver axis plays a significant role in liver disease progression (1). Whatever comes from the gut enters the liver through the portal circulation before returning to the heart via the hepatic vein. However, there exists a system of lymphatic channels in the gut, comprising of the intestinal and mesenteric lymphatic vessels with mesenteric lymph nodes that bypass the portal circulation in liver and directly connects the gut to the blood circulation via the thoracic duct. Gut lymphatics contain blind-ended lymphatic capillaries with a single layer of lymphatic endothelial cells (LyECs) in the duodenum (lacteals) while the contractile collecting vessels contain both the LyECs and smooth muscle cells in the mesentery (2). Gut lymphatic vessels play essential roles in the absorption and transportation of fat, maintaining fluid homeostasis, removing interstitial fluid, macromolecules, immune cells, and microbial debris from the intestine and returning them to the blood circulation, thereby preventing edema and abdominal ascites (3).

Increase in the number of lymphatic vessels or lymphangiogenesis has been stated to be a prominent feature of gut inflammation. Lymphangiogenesis in the gut during inflammation compensates for lymphatic insufficiency in patients with gut inflammatory diseases such as inflammatory bowel disease and Crohn's disease, where there is both an increase and redistribution of lymphatic vessels (4, 5). In liver cirrhosis, it is documented

that the production of abdominal lymph increases 30-fold and there exists a positive correlation of lymph flow with increasing portal pressures (6, 7). Using animal models of CCl4-induced liver damage, an elegant study has reported that mesenteric lymphatic vessels show an impaired phenotype and reduced contractility in cirrhosis (8). However, there are no human studies that have investigated intestinal lymphatic vessels in liver cirrhosis.

VEGF-C, a key pro-lymphangiogenic factor primarily guides gut lymphangiogenesis via binding to its tyrosine kinase receptor, vegfr3 (9). Therapies aimed at enhancing lymphangiogenesis and improving the lymphatic transport and function with pro-lymphangiogenic factors, such as VEGF-C has been shown to constitute an effective strategy to improve lymphatic drainage and ameliorate inflammation in diseases like rheumatoid arthritis, skin inflammation and hepatic encephalopathy (10-13). Use of pro-lymphangiogenic factors as therapeutic molecules for the restoration of gut lymphatic drainage in cirrhosis has not been explored. The short half-life and systemic side effects of these growth factors are some of the major hurdles that have limited their applications in the clinical arena (14).

In the current study, we characterized intestinal lymphatic vessels in patients with liver cirrhosis and also hypothesized a therapeutic role of pro-lymphangiogenic factor, VEGF-C in experimental models of liver cirrhosis and portal hypertension. To minimize the side effects of systemic delivery and increase the bioavailability of VEGF-C, we fabricated an engineered human VEGF-C gene by encapsulating it within lipocarriers and linking to vegfr3 antibody to ensure its lymphatic vessel-specific delivery for targeted gut lymphangiogenesis. We studied the effects of this nano-engineered molecule on

lymphatic vessels, lymphatic drainage in the mesentery, ascites, hepatic and systemic hemodynamics.

## Methods

### Patient Studies

**Study groups:** The study was approved by the Ethics Committee of Institute of liver and biliary Sciences (No. ILBS/AC/2018/11252/3215). Written informed consent was obtained from all subjects enrolled in the study. Patients were eligible for inclusion in this study if they had been diagnosed with liver cirrhosis (viral, alcoholic or NAFLD). The diagnosis of liver cirrhosis was established by means of histology and/or by its clinical, laboratory, endoscopic or imaging manifestations. The exclusion criteria were as follows: malignancy, diabetes mellitus, rheumatic diseases, tuberculosis, renal diseases, gastrointestinal diseases (e.g. celiac disease, inflammatory bowel disease, gastrointestinal bleeding in the last 4 weeks), intestinal surgery or INR > 2 (to avoid risk of bleeding during taking of biopsy). Patients with cirrhosis were subsequently divided into two groups: patients with decompensated cirrhosis (n = 13) or compensated cirrhosis (n = 12). Classification in decompensated or compensated disease was based on the presence or absence of ascites. The control group comprised of healthy individuals matched for age and sex, without any of the above-stated exclusion criteria, who underwent an upper gastrointestinal tract endoscopy without pathologic findings (n = 8). All subjects enrolled in the study underwent an upper gastrointestinal tract endoscopy, during which biopsies were obtained from the second portion of the duodenum (D2), distal to the ampulla of Vater. D2 biopsies were fixed in 10% neutral buffered formalin, embedded in paraffin, sectioned at 3-5 µm and stained with haematoxylin and eosin. In each sample, histologic features were studied, in a blind fashion, and recorded. Histologically, lymphatic vessels

in the duodenum were identified as thin-walled vessels consisting of a single layer of endothelial cells.

**Formulation and characterization of antibody anchored VEGF-C-engineered immuno-liponanocarriers:** Vegfr3 antibody anchored VEGF-C-engineered immunolipocarriers (E-VEGF-C) were formulated using cold High Shear Homogenization (HSH) technique. E-VEGF-C was systematically evaluated for mean particle size (z-average), polydispersity index (PDI) and zeta potential (ZP) analysis by dynamic laser light scattering (DLS). Detailed methods are explained in supplementary files.

***In vitro* Studies with LyECs**

The uptake of coumarin-6 labelled E-VEGF-C was monitored in the isolated and sorted podoplanin-positive (pdn+) mesenteric lymphatic endothelial cells (LyECs) as previously described (8).

***In vivo* Studies**

**Study Groups and treatment:** All animals received humane care according to the criteria outlined in the ‘‘Guide for the Care and Use of Laboratory Animals’’ prepared by the National Academy of Sciences and published by the National Institutes of Health (NIH publication 86-23 revised 1985). The study performed was duly approved by the Animal ethics committee of ILBS, New Delhi as per the standard guidelines (Ethics Protocol No: IAEC/ILBS/18/01). Studies were performed on thirty-six 8-week old male Wistar rats and twelve male 8-10 week old Sprague Dawley (SD) rats, weighing 250~300 g. Animals were randomized in three groups for the cirrhotic study: Healthy Control group (treated with saline), CCl4-V or vehicle group (CCl4 plus lipid nanocarriers alone

without VEGF-C plasmid) and E-VEGF-C group (CCl4 plus E-VEGF-C). Two groups were prepared in PPVL study. PPVL-vehicle (PPVL plus nanocarriers alone) and PPVL-E-VEGF-C (PPVL plus E-VEGF-C). The E-VEGF-C groups, received E-VEGF-C via oral route at a dose of 300 μg per kg body weight of the animal, via 3 injections during the 11$^{th}$ week in CCl4 animals and in PPVL animals, E-VEGF-C was administered via oral route at a dose of 300 μg of the construct per kg body weight of the animal, via 3 injections one day after the PPVL surgery. Animals were monitored for lymphatic vessel drainage by bodipy, CT scans, hemodynamics and sacrificed 48 h after the last dose of E-VEGF-C.

In addition to the above three groups, another two groups of animals were made to study the organ biodistribution of coumarin-6 labelled E-VEGF-C in control and CCl4 rats (n=4 each). Further, a third group was used for studying the plasma profile of E-VEGF-C in control rats. Detailed methods are provided in supplementary (Supp) information.

**RT-PCR and Western Blots:** RNA and protein extraction, RT-PCRs and Western blotting was done from the mesenteric tissues. Details of primers is given in Supp Table S1 and antibodies in Supp Table S2.

**Assessment of blood and lymphatic vessels by immunohistochemistry:** Intestinal (patients and animals) and mesenteric tissue samples (animals) were stained for different lymphatic and blood vessel markers. Details of the antibodies are given in Supp Table S2.

**Assessment of Hepatic and Systemic Hemodynamic Parameters:** Hepatic and Systemic Hemodynamic Parameters were measured 48 h after the last dose of the respective treatments as reported earlier (15).

**Computed tomography analysis: Computed tomography analysis:** Computed tomography (CT) examination was performed 48 h after the treatment to visualize ascites and validate the presence of decompensation in cirrhotic animals. The animals were evaluated using Somatom Definition AS plus 128 Acquisition 384 slice reconstruction (Siemens Healthineers, Forchheim, Germany).

## Results

### Vegfr3+ lymphatic vessels are dilated in patients with decompensated cirrhosis

Characteristics of the patient groups are summarized in Table 1. All patients with decompensated cirrhosis had ascites, whereas ascites was absent in all patients diagnosed with compensated cirrhosis. None of the patients had chylous ascites. The lymphatic vessels in patients were characterized by H & E and vegfr3 staining of the D2 biopsies. Histologically, patients with decompensated cirrhosis displayed a large number of dilated lymphatic channels in comparison to patients with compensated cirrhosis or healthy controls (Supp Figure 1). Vegfr3 protein expression was evident in the LyECs and was increased in decompensated as compared to compensated cirrhosis (Figure 1A, B). A marked dilation of vegfr3-positive lymphatic vessels was observed in the mucosal and submucosal regions in biopsies of decompensated cirrhosis compared to controls (Figure 1C). Multivariate analysis showed a significant positive correlation of vegfr3 IHC scores with the MELD-Na score (continuous variable, vegfr3= 0.82 + 0.37 x MELD) and the presence of ascites (categorical variable, r= 0.75, p= 0.001) (Figure 1D, E).

### E-VEGF-C for sustained and targeted delivery of VEGF-C in Vegfr3+ lymphatic endothelial cells

Based on the clinical correlation data, we hypothesized that increased number of dilated lymphatic vessels and lymph transport failure is associated with ascites in decompensated cirrhosis. Hence, enhancing the number of functional vegfr3+ lymphatic vessels (in the mesentery) by treating with lymphangiogenic factor, VEGF-C may improve lymphatic drainage in cirrhotic rats. To this end, we developed vegfr3-anchored E-VEGF-C-

engineered immuno-liponanocarriers for achieving targeted site-specific delivery of VEGF-C in the gut LyECs (Figure 2A). VEGF-C was engineered using immuno-liponanocarriers to achieve desired therapeutic efficacy of the active VEGF-C cargo. Next, these VEGF-C nanocarriers were conjugated with lymphatic endothelial ligand, vegfr3 to specifically achieve delivery of VEGF-C only in vegfr3-positive gut lymphatic vessels. The z-average particle size of the engineered VEGF-C (E-VEGF-C) was found to be 110.7 nm with a PDI value of 0.272 (Figure 2B). The zeta potential value of the E-VEGF-C-engineered immunolipo-nanocarriers before vegfr3 antibody incubation was found to be almost neutral (+1.12 mV) but inclined towards positive surface charge value (+6.52 mV), after vegfr3 antibody attachment (Figure 2C, D). This transition of shifting surface charge was confirmed improved stability of the immunolipo-nanocarriers after antibody attachment. The SEM image of E-VEGF-C immunolipocarriers images indicated cluster form of particles in nanoformat with desired size range. The immunolipocarriers could be seen forming agglomerates or lipid clusters due to sticky nature of lipoid S75 soybean phospholipids with 70% phosphatidylcholine (Figure 2E). TEM analysis of E-VEGF-C immunolipocarriers revealed them as irregular and scattered nanoparticles with desired nano size range below 200nm (Figure 2F). These observations were in accordance to DLS analysis.

To ensure if E-VEGF-C are internalized into the rat mesenteric LyECs, we first isolated and sorted the LyECs from rat mesenteric tissues. In the flow sorting assays, of the total population of cells, we obtained about 8.3% population of pdpn+ LyECs (Supp Figure 2A). We analyzed this population with pdpn antibody and obtained a purity of about 66.3% of pdpn+ LyECs (Supp Figure 2B). This population when cultured on fibronectin

coated plates stained intensely with pdpn antibody, further confirming their phenotype (Figure 3A, B). The LyECs were incubated with green coumarin-6-labelled E-VEGF-C. Fluorescence microscopy revealed an efficient internalization of E-VEGF-C by the LyECs at 4 h (Figure 3C, D).

**Tissue Bio-distribution and Toxicity of E-VEGF-C in vivo**

To investigate the specificity of E-VEGF-C delivery *in vivo*, biodistribution studies of E-VEGF-C were performed two hours post its oral administration by using spectroflourimetry, fluorescence microscopy and VEGF-C ELISAs in control and cirrhotic rats (Figure 4A). CCl4 cirrhotic rats showed increased levels of fluorescence and also E-VEGF-C in the mesenteric and duodenal tissues in comparison to the control animals ($P< 0.05$ each), with CCl4 mesenteric tissues showing the highest levels of all other groups (Figure 4B, C). Fluorescence and VEGF-C levels were also detected in other tissues in both control and CCl4 rats, which might also be due to the detection of endogenous rat VEGF-C levels (Figure 4B-D, Supp Figure S3A, B). In serum of control animals, levels of VEGF-C exhibited a biphasic peak, the first peak appeared at about 10 min, and the second peak at about 5 hours (Figure 4E). There was no adverse effect or mortality after E-VEGF-C treatment in either control or CCl4 rats (data not shown).

**E-VEGF-C treatment induces Lymphatic Vessel Proliferation and Improves Drainage**

We next studied the effects of E-VEGF-C treatment in the cirrhotic animals (Figure 5A). CCl4-V cirrhotic rats showed increased numbers of vegfr3+ dilated lymphatic vessels in

the both the duodenum and mesenteric tissues in comparison to the control rats (Supp Figure 4A-C). In E-VEGF-C treated animals, the dilated lymphatic channels were observed, albeit in comparison to the vehicle, there was increased vegfr3+ sprouts in both the duodenum and mesentery (Supp Figure 4B, C). We focused on the mesenteric lymphatic vessels particularly as they are known to play a key role in abdominal fluid homeostasis. We first analyzed the protein expression of human VEGF-C protein in the mesenteric tissues in different study groups. Results showed a significant increase in VEGF-C protein in the treated tissues as compared to the vehicle treated tissues (Figure 5B). To investigate active lymphangiogenesis in the mesenteric tissues, we studied expression of the Akt/pAkt and ERK/pERK proteins in different study groups. The expression of vegfr3, Akt and pAkt was not different among the vehicle and treated animals. As compared to the controls, the p-Akt/t-Akt was enhanced in both the vehicle and E-VEGF-C rats while that of pERK/ERK was substantially enhanced in the treated animals in comparison to that observed in the vehicle animals, indicating an activation of the lymphangiogenic pathways downstream of vegfr3 (Figure 5B). To validate lymphatic vessel proliferation, we performed a dual staining of vegfr3 and Ki67 in the mesenteric tissues of the animal groups. There was a significant increase in the number of Ki67+vegfr3+ LyECs in the mesentery in the treated E-VEGF-C treated rats as compared to that observed in the CCl4-V ($P< 0.05$) or control rats ($P< 0.001$) as seen by an increase in the number of dual positive vegfr3+Ki67+ LyECs (Figure 5C, D). To assess lymphatic drainage, we studied the functionality of the lymphatic vessels by measuring the amount of gavaged bodipy in the mesenteric vessels in the study groups. Quantification in the mesenteric tissue homogenates showed decreased bodipy fluorescence after 2 h of

administration in CCl4-V rats as compared to that in the control animals (Figure 5E, F). E-VEGF-C treated CCl4-V rats revealed a significant increase in flourescence as compared to that seen in the vehicle rats with respect to the controls ($P< 0.05$, Figure 5E, F).

**E-VEGF-C reduces Ascites and ameliorates Portal Pressure in Cirrhotic and Non-Cirrhotic Portal Hypertensive Rats**

We then investigated whether an improvement in lymphatic drainage and a reduction in mesenteric inflammation was associated with a reduction in ascitic fluid volume in the E-VEGF-C treated cirrhotic rats. No ascites was observed in the control group, whereas all the CCl4-V cirrhotic rats displayed severe ascites in our study. At the end of treatment, we assessed the volume of peritoneal fluid in the CCl4-V and E-VEGF-C groups. E-VEGF-C rats displayed a marked reduction in the ascites volume as compared to that observed in CCl4-V rats as was also clearly evident in CT scan slices of the two groups ($P< 0.001$, Figure 6A, B). Along with ascites reduction, evans blue analysis showed a significant increase in plasma volume in cirrhotic rats treated with E-VEGF-C compared with vehicle animals ($P< 0.05$, Figure 6C).

Next, we analyzed if this reduction in the ascitic fluid volume after E-VEGF-C treatment was also associated with changes in liver physiology and pathology. Intraperitoneal CCl4 treatment for 10 weeks markedly increased portal pressure (PP) in the rats in comparison to that of the control rats (Figure 6D). E-VEGF-C treatment, however significantly attenuated the PP as compared to the vehicle treated rats ($P< 0.001$, Figure 6D). To ascertain if the observed reduction in PP was due to a change in the portal blood flow

(PBF) or intrahepatic resistance (IHR), we also monitored these parameters in all the study groups. E-VEGF-C treatment significantly decreased the PBF, in turn increasing the mean arterial pressure (MAP) as compared to that of the CCl4-V cirrhotic rats (Figure 5D, Supp Figure S5). The IHR in E-VEGF-C treated rats was however similar to that of the cirrhotic rats. In comparison to control rats, liver weights in E-VEGF-C rats and CCl4-V rats were also similar (Supp Figure S5). We next evaluated changes in histological and biochemical parameters of liver in the cirrhotic animals. Masson's trichrome staining of the liver tissues revealed that both E-VEGF-C and vehicle rats showed Ishak's fibrosis scores of 5/6 or 6/6 depicting complete cirrhosis (thick fibrous septa or many minute nodules) (Figure 6E). In terms of biochemical parameters, CCl4 treatment resulted in a significant increase in serum ALT levels and a decrease in albumin levels as compared to the control group (Supp Table S3). There was no significant improvement in levels of serum albumin and ALT in the E-VEGF-C treated rats as compared to that seen in CCl4 rats. The kidney functions tests were in normal ranges in all the study groups (Supp Table S3).

Next, we investigated the expression of important genes known to be associated with VEGF-C expression in the mesentery. Of all the factors analyzed, mesenteric tissues in E-VEGF-C treated rats showed a marked increment in the expression of the chemokine, CCL21 ($P < 0.05$, Figure 6F). Interestingly, the pro-inflammatory gene, iNOS instead showed a significant reduction in their expression in E-VEGF-C treated rats in comparison to that observed in the CCl4-V rats ($P < 0.05$ for each, Figure 6F).

We also assessed levels of TNF-α and endotoxins in the ascitic fluid and in the serum. Serum endotoxins and TNF-α levels were considerably enhanced in CCl4-V cirrhotic rats in comparison to that present in control rats (Figure 6G, I). We did not observe any significant change in the serum endotoxin and TNF-α levels in the E-VEGF-C treated rats in comparison to that observed in the CCl4-V rats (Figure 6G, I). In the ascitic fluid, there was no significant decrease in the levels of endotoxins and TNF-α in the E-VEGF-C treated rats vis a vis CCl4-V cirrhotic rats in terms of per ml units. Nevertheless, a substantial reduction in the ascitic fluid volume per se in E-VEGF-C treated rats resulted in an overall decrease in the levels of these entities in the abdomen (Figure 6H, J).

Given the fact that VEGF-C also participates in blood vessel angiogenesis in some tissues, we also evaluated if E-VEGF-C had any effects on the mesenteric tissue blood vessels and inflammation. The mesenteric tissues displayed significant increase in the number of CD31-positive blood vessels in both CCl4-V and E-VEGF-C rats as compared to that observed in the controls ($P < 0.001$ each, Supp Figure S6A, B). We did not find any significant difference in the number of CD31-positive vessels between CCl4-V and E-VEGF-C rats (Supp Figure S6A, B). In the E-VEGF-C rats, however inflammation was considerably reduced in the mesenteric tissues in comparison to that present in the CCl4-V rats (Supp Figure 6C).

**E-VEGF-C reduces Portal Pressure in Non-Cirrhotic Portal Hypertensive Rats**

We next probed if E-VEGF-C treatment improved PP irrespective of liver cirrhosis, by measuring the hepatic hemodynamics in non-cirrhotic portal hypertensive (PPVL) animals (Figure 7A). Histology of these animals displayed portal inflammation in liver

but no significant fibrosis (Supp Figure S7A). PPVL animals treated with E-VEGF-C also displayed an increased VEGF-C and pERK/t-ERK protein expression in comparison to that seen in the vehicle rats (Figure 7B). Increased numbers of vegfr3+ dilated lymphatic channels were well evident in the duodenal tissues in the PPVL animals (Figure 7C, Supp Figure S7B, C). The dilated channels were also observed in the E-VEGF-C treated PPVL animals. In the mesentery, E-VEGF-C treated PPVL rats showed an increased presence of vegfr3+ lymphatic vessels vis-à-vis the vehicle animals (Figure 7C). Hemodynamic analysis depicted a significant reduction in the PP and PBF of PPVL animals treated with E-VEGF-C in comparison to that observed in vehicle animals ($P< 0.001$, Figure 7D). The expression of bFGF, CCL21, iNOS and eNOS was significantly higher in the mesentery of the PPVL vehicle animals in comparison to the controls (Figure 7E). In E-VEGF-C treated PPVL rats, there was a significant reduction of iNOS as compared to the vehicle animals ($P< 0.05$, Figure 7E).

## Discussion

In the current study, we characterize and report significantly increased number of dilated vegfr3+ duodenal lymphatic vessels in patients with decompensated cirrhosis with both mucosal and submucosal involvement, clearly implying gut lymphatic dysfunction similar to that seen in intestinal lymphangectasia and gut inflammatory disorders (16, 4, 5). An increase in the expression of vegfr3-postive vessels in patients with decompensated cirrhosis may be attributed as a compensatory lymphangiogenesis response by the gut lymphatic vessels (17, 18). The presence of ascites in these patients was the most significant correlate of dilated lymphatic channels corroborating the fact that the impairment of intestinal lymphatic function and drainage represents one of the key factors affecting fluid accumulation into the peritoneal cavity in cirrhosis (7).

Similar to patients with decompensated cirrhosis, we observed enhanced numbers of dilated vegfr3+ lymphatic vessels in the duodenal and mesenteric tissues of the experimental cirrhotic animals, suggestive of an increased but insufficient lymphangiogenesis to compensate the increased fluid load and inflammation. However, most of these vessels were dilated. A previous study in cirrhotic rats documented that an increased expression of eNOS in the mesenteric LyECs was the cause of dysfunctional lymphatic drainage in cirrhosis and that inhibiting eNOS improved the lymphatic transport of the existing vessels by increasing contractile activity of these vessels (8). In our study, instead of manipulating the contractile activity of the existing mesenteric lymphatic vessels by using eNOS inhibitor, we focused on increasing the numbers of new lymphatic channels via VEGF-C treatment. To minimize the systemic toxic effects of

VEGF-C, we designed our therapeutic VEGF-C molecule using nanolipocarriers. A recent report illustrated the therapeutic potential of the fully human fusion protein, F8-VEGF-C (VEGF-C linked to F8 antibody) for a targeted delivery of VEGF-C in mouse models of chronic inflammatory skin disease. However, the study did not report a sustained release of VEGF-C (19). We used various strategies in this study to ensure a targeted and sustained delivery of VEGF-C in the lymphatic channels. We used immunolipo-nanocarriers so that similar to chylomicrons they take up the lymphatic route *in vivo*. Engineered lipid-mediated matrix system allows the release of the cargo in such a way that the loading dose is achieved within a shorter period to initiate the pharmacodynamic action (20). The use of lipid nanocarriers also permits the cargo from the E-VEGF-C to be released in a sustained and programmable manner. Then, given an increased expression of vegfr3+ in gut LyECs, we used vegfr3 antibody to tag VEGF-C for a targeted delivery to the gut lymphatic vessels. The in vitro uptake studies clearly depicted more than 90% uptake of the E-VEGF-C by the LyECs.

In the *in vivo* biodistribution studies, cirrhotic rats had maximum levels of E-VEGF-C in the duodenum and in the mesenteric tissues. The dose of human VEGF-C construct used in our study was half the dose that has been used in the earlier study (19). In the plasma, the drug (human VEGF-C) release pattern in E-VEGF-C formulation followed a biphasic release behavior. The initial burst release of the drug observed at 10 min might be due to presence of adsorbed drug on the surface of nanoparticles, while the second peak at 5 h, depicting sustained release of drug might be due to increased diffusional distance and hindering effects by the surrounding solid lipid shell.

Treatment with E-VEGF-C markedly enhanced the expression of VEGF-C and pERK proteins in the mesentery, indicating VEGF-C-driven proliferation in the LyECs. Functionally, both MAP/ERK and PI3k/Akt pathways play important roles in regulating the sprouting and proliferation/survival of LyECs respectively (21). We observed a predominance of the MAP/ERK pathway over the Akt pathway participating in the lymphatic vessel proliferation in the mesenteric tissues of the treated animals (21). Also, our treatment significantly improved the lymphatic drainage and function of the vessels. This is in accordance with many previous studies that have shown drainage-promoting function of VEGF-C in experimental models of bacterial skin inflammation and inflammatory bowel disease (22, 23). An improvement in lymphatic drainage and functionality of the new vessels in CCl4 cirrhotic rats formed was well evident by a marked reduction in the ascitic fluid volume in rats with fully developed ascites. A decrease in ascites was accompanied by an increase in the plasma volume of the treated rats suggesting that there may be reabsorption of ascites into the circulating blood (7). Along with a reduction in ascites, there was also a significant decrease in the PP in cirrhotic portal hypertensive rats treated with E-VEGF-C, which was associated with attenuated PBF and increased MAP. There was however no change in the IVR, indicating that improvement in PBF and not the hepatic resistance (fibrosis) lead to an improvement in portal pressure after treatment. A decrease in PP may be caused by a reduction in the intra-abdominal pressure that might have occurred during removal of ascitic fluid into newly formed lymphatic vessels. It has been postulated that removal of ascites plays a role in the postparacentesis systemic hemodynamic changes through mechanical decompression of the splanchnic vascular bed (24). However, a reduction in PP due to an

increase in the number of lymphatic vessels and a decrease in the interstitial fluid pressure may also have led to a decrease in ascites (25). Intriguingly, this decrease in PP and ascites was also observed in the non-cirrhotic PPVL animals after E-VEGF-C treatment, validating the favorable effects of the pro-lymphangiogenic treatment on PBF and systemic hemodynamics. An improvement in the PP was not associated with a significant improvement in liver pathology in the treated rats, stipulating that there are no direct protective effects of E-VEGF-C treatment on the hepatic compartment per se. We also did not observe any major changes in the serum albumin and ALT levels in the treated animals. In our study, we have given a therapeutic E-VEGF-C treatment in decompensated animals after 10 weeks of treatment, when liver cirrhosis and ascites had already set in. It would be worthwhile to evaluate the effects of E-VEGF-C on the early onset of decompensation and liver pathology in compensated cirrhotic models of portal hypertension using a preventive treatment approach.

Mesenteric angiogenesis marked by an increase in CD31+ vessels is a common feature of cirrhosis, and this was also observed in cirrhotic rats (26). However, we did not detect any significant changes in the density of CD31+ blood vessels in E-VEGF-C–treated rats, reflecting that VEGF-C did not affect the mesenteric blood vessels analogous to that has been documented earlier (22, 23). With respect to inflammation, there was a conspicuous decrease in mesenteric tissue inflammation in histological analysis and both bacterial endotoxin and TNF-α levels in the ascitic fluids of the treated animals. The mesenteric expression of pro-inflammatory genes such as iNOS was also downregulated after E-VEGF-C treatment in both cirrhotic and PPVL animals. It has been reported formerly that during inflammation an increase in iNOS-expressing inflammatory cells significantly

reduce lymphatic contraction (27). Thus, a reduction of iNOS expression in E-VEGF-C rats is also expected to have a beneficial effect on the contractility and lymphatic drainage of the existing lymphatic channels in E-VEGF-C treated rats (28). Most striking was the increase in the gene expression of CCL21 in E-VEGF-C rats, demonstrating that the newly formed lymphatic vessels are also capable of augmenting the production of chemoattractants and possibly also enhancing the mobilization of CCR7-positive dendritic cells to the draining lymph nodes (29). An earlier study documented that stimulation of cardiac lymphangiogenesis with VEGF-C improved the trafficking of immune cells to draining lymph nodes after myocardial infarction (30). It would be worthwhile to study immune modulation in the mesenteric tissues and lymph nodes by VEGF-C treatment in the cirrhotic models.

With respect to eNOS, previous studies have illustrated an increase in the expression of phosphorylated eNOS due to an activation of PI3Kinase/Akt signaling in LyECs after VEGF-C treatment (31). Also, eNOS inhibition has shown to cause a decreased lymphatic fluid velocity, and NO donors have a favorable effect specifically on the collecting lymphatic vessels (32). We did not observe a significant change in the eNOS gene expression in the treated animals but a limitation of our study is that we have not estimated the eNOS signaling pathway specifically in the LyECs after VEGF-C treatment, which thus warrants further investigations. Given the fact that the agonists of the eNOS pathway such as statins that work by attenuating hepatic microvascular dysfunction have evolved as a choice of therapy for portal hypertension (33, 34), it would be interesting to evaluate their effects on the mesenteric lymphatic vessels and drainage in portal hypertension.

To summarize, our study reports increased number of markedly dilated duodenal lymphatic vessels in patients with decompensated cirrhosis. The study underscores the use of a nanoengineered VEGF-C as a lymphangiogenic growth factor for enhancing gut/mesenteric lymphangiogenesis and improving lymphatic drainage by providing an efficient exit route for ascitic fluid, further strengthening the concept of gut-liver axis (Figure 8). The study proposes pro-lymphangiogenesis as an innovative and targeted strategy for the management of ascites and portal hypertension.

## Competing Interests

The authors declare no competing interests.

## References

1. Albillos A, de Gottardi A, Rescigno M. The gut-liver axis in liver disease: Pathophysiological basis for therapy. J Hepatol. 2020;72:558-77.
2. Miller MJ, Newberry RD. Microanatomy of the intestinal lymphatic system. Annals of the New York Academy of Sciences. 2010;1207:E21.
3. Bernier-Latmani J, Petrova TV. Intestinal lymphatic vasculature: structure, mechanisms and functions. Nature Reviews Gastroenterology & Hepatology. 2017;14:510
4. Becker F, Yi P, Al-Kofahi M, Ganta VC, Morris J, Alexander JS. Lymphatic dysregulation in intestinal inflammation: new insights into inflammatory bowel disease pathomechanisms. Lymphology. 2014;47:3-27.
5. Danese S. Role of the vascular and lymphatic endothelium in the pathogenesis of inflammatory bowel disease:'brothers in arms'. Gut. 2011;60:998-1008.
6. Dunbar BS, Elk JR, Drake RE, Laine GA. Intestinal lymphatic flow during portal venous hypertension. American Journal of Physiology-Gastrointestinal and Liver Physiology. 1989;257:G94-8.
7. Chung C, Iwakiri Y. The lymphatic vascular system in liver diseases: its role in ascites formation. Clinical and molecular hepatology. 2013;19:99.
8. Ribera J, Pauta M, Melgar-Lesmes P, Tugues S, Fernández-Varo G, Held KF, Soria G, Tudela R, Planas AM, Fernández-Hernando C, Arroyo V. Increased nitric oxide production in lymphatic endothelial cells causes impairment of lymphatic drainage in cirrhotic rats. Gut. 2013;62:138-45.

9. Nurmi H, Saharinen P, Zarkada G, Zheng W, Robciuc MR, Alitalo K. VEGF-C is required for intestinal lymphatic vessel maintenance and lipid absorption. EMBO molecular medicine. 2015;7:1418-25.
10. Güç E, Briquez PS, Foretay D, Fankhauser MA, Hubbell JA, Kilarski WW, Swartz MA. Local induction of lymphangiogenesis with engineered fibrin-binding VEGF-C promotes wound healing by increasing immune cell trafficking and matrix remodeling. Biomaterials. 2017;131:160-75.
11. Bouta EM, Bell RD, Rahimi H, Xing L, Wood RW, Bingham III CO, Ritchlin CT, Schwarz EM. Targeting lymphatic function as a novel therapeutic intervention for rheumatoid arthritis. Nature Reviews Rheumatology. 2018;14:94.
12. Hagura A, Asai J, Maruyama K, Takenaka H, Kinoshita S, Katoh N. The VEGF-C/VEGFR3 signaling pathway contributes to resolving chronic skin inflammation by activating lymphatic vessel function. Journal of dermatological science. 2014;73:135-41.
13. Hsu SJ, Zhang C, Jeong J, Lee SI, McConnell M, Utsumi T, Iwakiri Y. Enhanced meningeal lymphatic drainage ameliorates neuroinflammation and hepatic encephalopathy in cirrhotic rats. Gastroenterology. 202;:S0016-5085:35439-1
14. Lohela M, Saaristo A, Veikkola T, Alitalo K. Lymphangiogenic growth factors, receptors and therapies. Thrombosis and haemostasis. 2003;90:167-84.
15. Tripathi DM, Vilaseca M, Lafoz E, Garcia-Calderó H, Haute GV, Fernández-Iglesias A, de Oliveira JR, García-Pagán JC, Bosch J, Gracia-Sancho J. Simvastatin prevents progression of acute on chronic liver failure in rats with cirrhosis and portal hypertension. Gastroenterology. 2018;155:1564-77.

16. Vignes S, Bellanger J. Primary intestinal lymphangiectasia (Waldmann's disease). Orphanet journal of rare diseases. 2008;3:5.

17. Rahier JF, De Beauce S, Dubuquoy L, Erdual E, Colombel JF, Jouret-Mourin A, Geboes K, Desreumaux P. Increased lymphatic vessel density and lymphangiogenesis in inflammatory bowel disease. Alimentary pharmacology & therapeutics. 2011;34:533-43.

18. Linares PM, Gisbert JP. Role of growth factors in the development of lymphangiogenesis driven by inflammatory bowel disease: a review. Inflammatory bowel diseases. 2011;17:1814-21.

19. Schwager S, Renner S, Hemmerle T, Karaman S, Proulx ST, Fetz R, Golding-Ochsenbein AM, Probst P, Halin C, Neri D, Detmar M. Antibody-mediated delivery of VEGF-C potently reduces chronic skin inflammation. JCI insight. 2018;3.

20. Banerjee S, Pillai J. Solid lipid matrix mediated nanoarchitectonics for improved oral bioavailability of drugs. Expert opinion on drug metabolism & toxicology. 2019;15:499-515.

21. Deng Y, Zhang X, Simons M. Molecular controls of lymphatic VEGFR3 signaling. Arterioscler Thromb Vasc Biol. 2015;35:421-9.

22. D'alessio S, Correale C, Tacconi C, Gandelli A, Pietrogrande G, Vetrano S, Genua M, Arena V, Spinelli A, Peyrin-Biroulet L, Fiocchi C. VEGF-C–dependent stimulation of lymphatic function ameliorates experimental inflammatory bowel disease. The Journal of clinical investigation. 2014;124:3863-78.

23. Visuri MT, Honkonen KM, Hartiala P, Tervala TV, Halonen PJ, Junkkari H, Knuutinen N, Ylä-Herttuala S, Alitalo KK, Saarikko AM. VEGF-C and VEGF-C156S in the pro-lymphangiogenic growth factor therapy of lymphedema: a large animal study. Angiogenesis. 2015;18:313-26.

24. Cabrera J, Falcon L, Gorriz E, Pardo MD, Granados R, Quinones A, Maynar M. Abdominal decompression plays a major role in early postparacentesis haemodynamic changes in cirrhotic patients with tense ascites. Gut. 2001;48:384-9.

25. Aukland K, Reed RK. Interstitial-lymphatic mechanisms in the control of extracellular fluid volume. Physiological reviews. 1993;73:1-78.

26. Geerts AM, De Vriese AS, Vanheule E, Van Vlierberghe H, Mortier S, Cheung KJ, Demetter P, Lameire N, De Vos M, Colle I. Increased angiogenesis and permeability in the mesenteric microvasculature of rats with cirrhosis and portal hypertension: an *in vivo* study. Liver Int. 2006;26:889-98.

27. Chakraborty S, Zawieja SD, Wang W, Lee Y, Wang YJ, von der Weid PY, Zawieja DC, Muthuchamy M. Lipopolysaccharide modulates neutrophil recruitment and macrophage polarization on lymphatic vessels and impairs lymphatic function in rat mesentery. American Journal of Physiology-Heart and Circulatory Physiology. 2015;309:H2042-57.

28. Torrisi JS, Hespe GE, Cuzzone DA, Savetsky IL, Nitti MD, Gardenier JC, Nores GD, Jowhar D, Kataru RP, Mehrara BJ. Inhibition of inflammation and iNOS improves lymphatic function in obesity. Scientific reports. 2016;6:19817.

29. Russo E, Nitschké M, Halin C. Dendritic cell interactions with lymphatic endothelium. Lymphatic research and biology. 2013;11:172-82.

30. Vieira JM, Norman S, Villa Del Campo C, Cahill TJ, Barnette DN, Gunadasa-Rohling M, Johnson LA, Greaves DR, Carr CA, Jackson DG, Riley PR. The cardiac lymphatic system stimulates resolution of inflammation following myocardial infarction. J Clin Invest. 2018;128:3402-3412.

31. Coso S, Zeng Y, Opeskin K, Williams ED. Vascular endothelial growth factor receptor-3 directly interacts with phosphatidylinositol 3-kinase to regulate lymphangiogenesis. PLoS One. 2012;7:e39558.

32. Hagendoorn J, Padera TP, Kashiwagi S, Isaka N, Noda F, Lin MI, Huang PL, Sessa WC, Fukumura D, Jain RK. Endothelial nitric oxide synthase regulates microlymphatic flow via collecting lymphatics. Circ Res. 2004;95:204-9.

33. Wiest R, Groszmann RJ. The paradox of nitric oxide in cirrhosis and portal hypertension: too much, not enough. Hepatology. 2002;35:478-91.

34. Brusilovskaya K, Königshofer P, Schwabl P, Reiberger T. Vascular Targets for the Treatment of Portal Hypertension. Semin Liver Dis. 2019;39:483-501.

**Table 1: Characteristics of patients used in the study**

| **Parameters** | **Decompensated (13)** | **Compensated (12)** | **Controls (8)** |
|---|---|---|---|
| **Age (**mean±SD, yr.) | 53.8 ± 9.25 | 55.4 ± 10.01 | 47 ± 11.3 |
| **Gender** | 9M, 4F | 9M, 3F | 5M, 3F |
| **Aetiology of cirrhosis (Alcohol/NASH/Viral)** | 4/8/1 | 2/9/1 | - |
| **INR** | 1.8 ± 0.5 | 1.3 ± 0.2 | 1.1 ± 0.2 |
| **Serum albumin (g/dL)** | 3.0 + 0.3 | 3.2 + 0.49 | 4.2 + 0.19 |
| **Total bilirubin (mg／dL)** | 2.68 ± 1.1 | 1.32 ± 0.5 | 0.8 ± 0.4 |
| **Platelets** | 108.3 ± 50.9 | 136.4 ± 64.8 | 213 ± 61.5 |
| **Presence of Ascites (n/n)** | 13/13 | 0/12 | - |
| **MELD-Na Score** | 20.23 ± 1.8 | 10.9 ± 1.99 | - |

INR: international normalized ratio; MELD: Model for End-Stage Liver Disease

## Figure Legends

**Figure 1: Duodenal lymphatic channels in cirrhotic patients** (A) Representative vegfr3 immunohistochemical (IHC) stained sections (20x) of duodenal (D2) biopsies in controls (n=8) and patients with compensated cirrhosis (comp cirr, n=12) and decompensated cirrhosis (decomp cirr, n=13). Lymphatic vessels are shown by dotted lines. (B) Bar diagrams showing average number of vegfr3-positive lymphatic vessels per field in the study groups (n=8 each). (C) Bar diagrams showing average diameter of vegfr3-positive lymphatic vessels per field in the study groups (n=8 each). (D) Univariate and multivariate correlation between continuous clinical parameters of cirrhotic patients and number of vegfr3 positive dilated vessel channels in IHC (vegfr3 IHC score). Correlation of vegfr3 IHC score with categorical variable (presence of ascites) in cirrhotic patients is given. 'r' is Pearson's correlation co-efficient. Data represents mean $\pm$ standard deviation. '*' represents $p < 0.05$ and '**' represents $p < 0.001$. MELD: Model for End-Stage Liver Disease.

**Figure 2**: **Properties of nanoengineered VEGF-C (E-VEGF-C).** (A) A schematic representation of vegfr3-tagged VEGF-C nano-lipocarriers (E-VEGF-C). (B) Mean particle size of E-VEGF-C immunolipo-nanocarriers (C) Mean zeta potential value of E-VEGF-C immunolipo-nanocarriers without vegfr3 antibody (D) Mean zeta potential value with vegfr3 antibody. Different coloured peaks in the graphs are representing different replicates of samples. (E) SEM analysis of E-VEGF-C immunolipo-nanocarriers after incubation with vegfr3 antibody. (F) TEM analysis of E-VEGF-C after incubation with vegfr3 antibody.

**Figure 3: Invitro studies of lymphatic endothelial cells (LyECs) with E-VEGF-C. (A) Culture of Podoplanin (Pdpn)-positive LyECs after flow sorting (20x). (B)** Fluorescent images (20x) showing Pdpn positivity of the sorted LyECs. (C) Fluorescent images (20x) showing uptake of coumarin-6 labeled E-VEGF-C by LyECs at 60 min and 240 min (D) Line graph depicting the percentage of coumarin-positive cells (flourescence) at different time points.

**Figure 4: *In vivo* biodistribution studies after 2 hours of E-VEGF-C treatment.** (A) Schema of in vivo biodistribution studies. (B) Relative fluorescence units (flourescence intensity at 520 nm) of coumarin-6 tagged E-VEGF-C in control and CCl4 animals. (C) Representative flourescence images (4x) of E-VEGF-C in the mesentery. (D) Human VEGF-C levels (pg/mg total protein) in different tissues in control and CCl4 animals. (E) Levels of human VEGF-C (pg/ml) in rat plasma samples at indicated time points in control animals. Data represents mean $\pm$ standard deviation. N=4 each. '*' represents $p< 0.05$ and '**' represents $p< 0.001$.

**Figure 5: Effect of E-VEGF-C treatment on mesenteric lymphatic vessels in cirrhotic animal models of portal hypertension.** (A) Schema of the in vivo studies (B) Expression of different proteins in the mesenteric tissues of control, CCl4-V and E-VEGF-C treated rats as determined by Western blots and normalized to GAPDH. Data represents mean $\pm$ standard deviation. N=4 each. '*' represents $p< 0.05$. (C) Representative fluorescent images (20x) of Ki67 and vegfr3 dual positive lymphatic channels in the mesenteric tissues of control, CCl4-V and E-VEGF-C rats. Nuclei were

stained with DAPI. (D) Bar diagrams showing the average number of Ki67 and vegfr3 dual positive lymphatic vessels (network circles) in the mesentery of different study groups. Data represents mean ± standard deviation. N=6 each. '*' represents $p < 0.05$ and '**' represents $p < 0.001$. (E) Confocal images (40x) showing bodipy labeling in the mesenteric lymphatic channels. Images were taken after 2h of oral administration of bodipy (F) Bar diagram depicting relative change in bodipy fluorescence in CCl4-V and E-VEGF-C rats with respect to controls. Data represents mean ± standard deviation. N=4 each. '*' represents $p < 0.05$, '**' represents $p < 0.001$.

**Figure 6: Effect of E-VEGF-C treatment on ascitic fluid and liver physiology in cirrhotic animal models of portal hypertension.** (A) Representative computed tomographic (CT) scan slices showing abdominal cavity of the study groups. The regions of interest are marked with red dotted outline and correspond to the zones with accumulation of liquid. (B) Dot plots showing ascitic fluid volume (ml) in the study groups. (C) Histograms showing plasma volumes (ml) in the study groups measured using the Evans Blue dye dilution technique. Data represents mean ± standard deviation. N=4 each. (D) Bar Diagrams showing hepatic hemodynamic parameters, Portal pressure (PP), Portal Blood Flow (PBF) and Intrahepatic resistance (IHR) in the control, CCl4-V cirrhotic and E-VEGF-C rats. Data represents mean ± standard deviation. N=6 each. '*' represents $p < 0.05$ and '**' represents $p < 0.001$. (E) Masson Trichrome stained images (10x) of liver tissues in controls, CCl4-V and E-VEGF-C rats. Liver fibrosis was assessed using Laennec fibrosis scoring system. (F) Relative expression of genes in CCl4-V and E-VEGF-C rats with respect to controls in

the mesenteric tissues. Data represents mean ± standard deviation. N=4 each. '*' represents p< 0.05 and '**' represents p< 0.001. Dot plots showing levels of (G) Endotoxins (EU/ml) in the serum (H) Endotoxins (EU/ml) in the ascitic fluid (I) TNF-α (pg/ml) in serum (J) TNF-α (pg/ml) in the ascitic fluid. '*' represents p< 0.05 and '**' represents p< 0.001.

**Figure 7: Effect of E-VEGF-C treatment on mesenteric lymphatic vessels and liver physiology in the non-cirrhotic animal models of portal hypertension.** (A) Schema of the studies (B) Expression of different proteins in the mesenteric tissues of control (C), PPVL-VEH and PPVL + E-VEGF-C treated rats as determined by Western blot and normalized to GAPDH. Data represents mean ± standard deviation. N=4 each. '*' represents p< 0.05. (C) Vegfr3+ immunohistochemistry (20x) in the duodenal and mesenteric tissue sections of PPVL-VEH and PPVL + E-VEGF-C rats. (D)

Bar Diagrams showing hepatic hemodynamic parameters, Portal pressure (PP), Portal Blood Flow (PBF) and Intrahepatic resistance (IHR) in the non-cirrhotic PPVL rats treated with vehicle and that treated with E-VEGF-C. Data represents mean ± standard deviation. N=6 each. '*' represents p< 0.05 and '**' represents p< 0.001. (E) Relative expression of genes in PPVL-VEH and PPVL + E-VEGF-C rats with respect to controls in the mesenteric tissues. Data represents mean ± standard deviation. N=4 each. '*' represents p< 0.05.

**Figure 8:** Summary of the study.

Figure 1

(A)

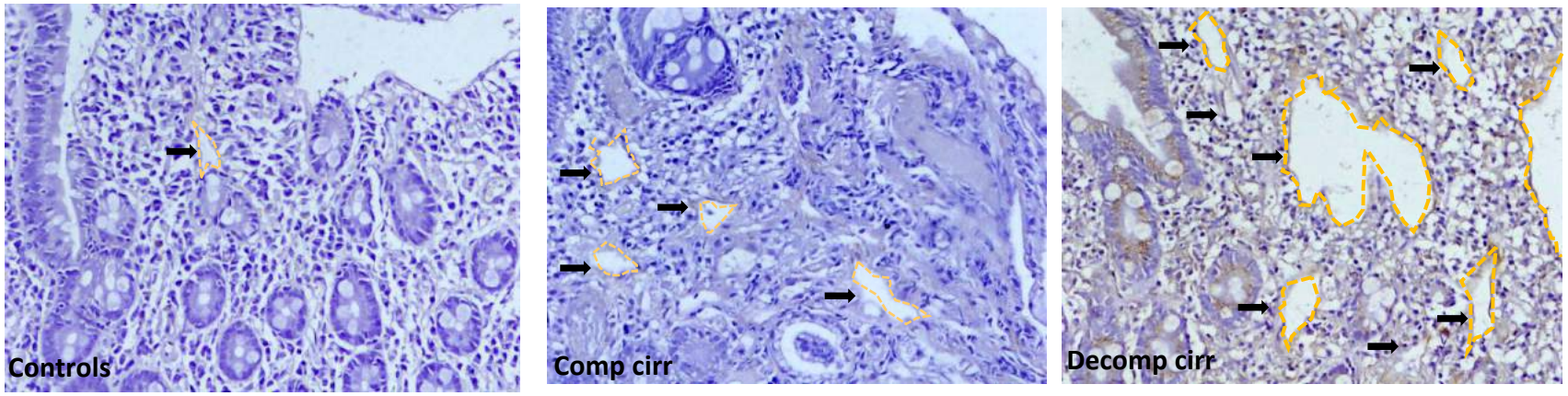
Controls
Comp cirr
Decomp cirr

(B)

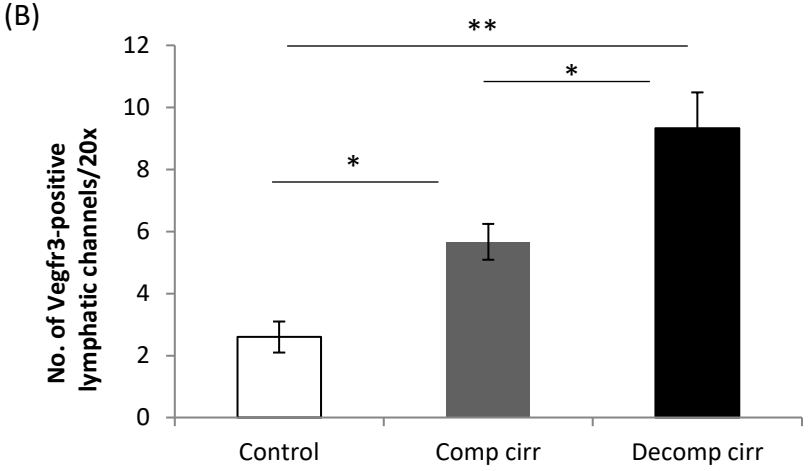
No. of Vegfr3-positive lymphatic channels/20x
12
10
8
6
4
2
0
**
*
*
Control
Comp cirr
Decomp cirr

(C)

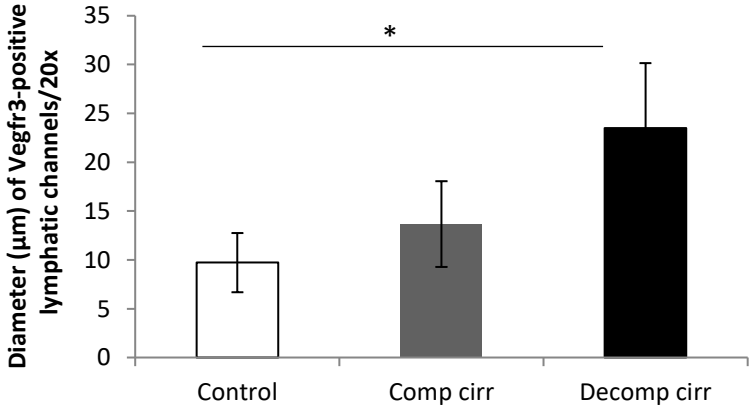
Diameter (µm) of Vegfr3-positive lymphatic channels/20x
35
30
25
20
15
10
5
0
*
Control
Comp cirr
Decomp cirr

Figure 1

(D)

**Univariate Analysis**

| Parameters | Correlation coefficient (r) (with vegfr3 IHC score) | p value |
|---|---|---|
| MELD-Na | 0.90 | 0.001** |
| Platelets/L | 0.15 | 0.57 |
| ALT (IU/L) | 0.46 | 0.08 |
| AST (IU/L) | 0.74 | 0.001** |
| Sodium | -0.47 | 0.07 |
| Albumin | -0.63 | 0.01* |

**Multivariate Analysis**

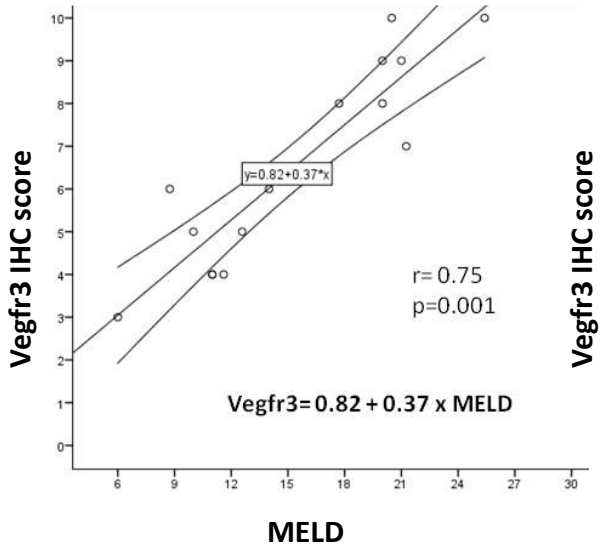


(E)

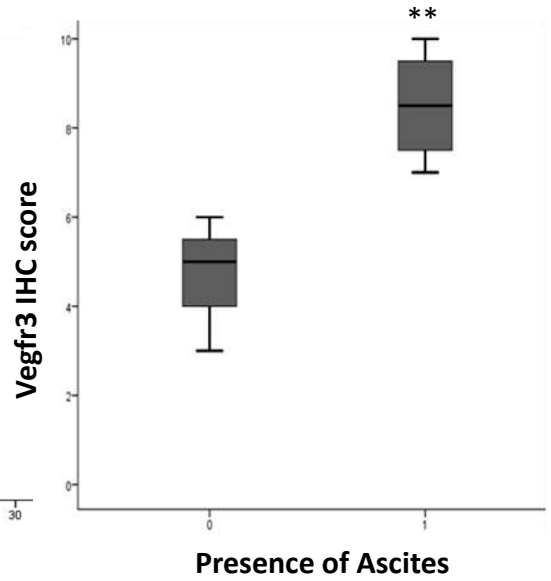

Figure 2

(A)

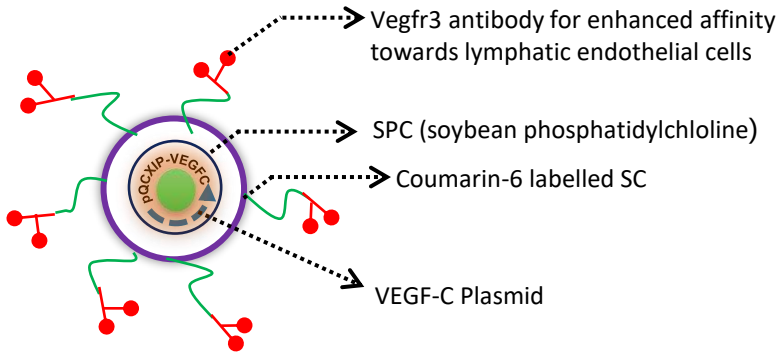


(B)

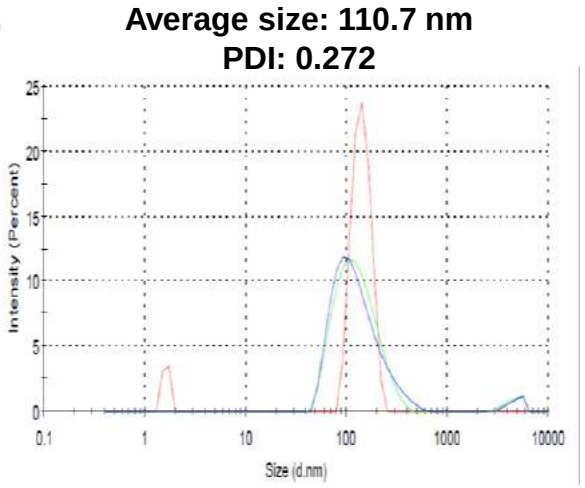


(C)

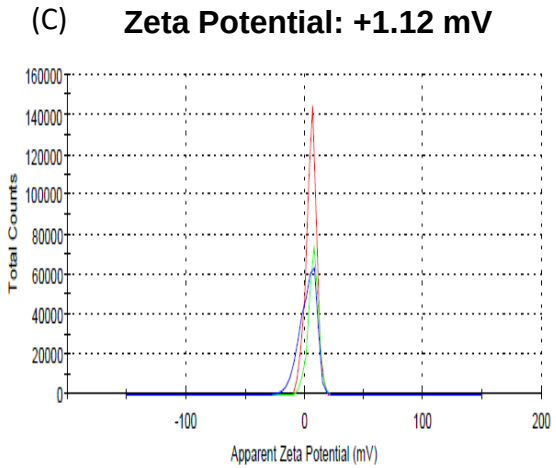


(D)

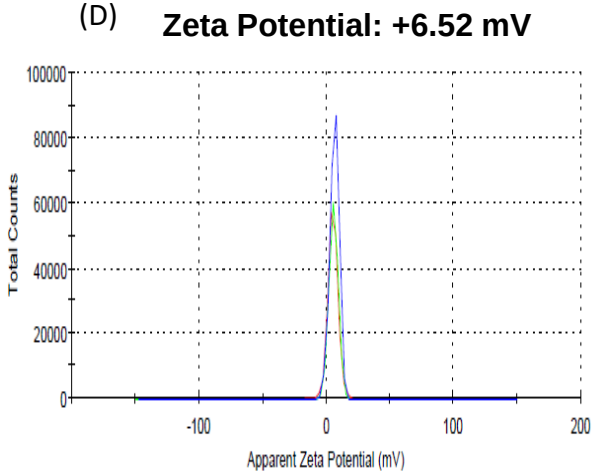

Figure 2

(E)

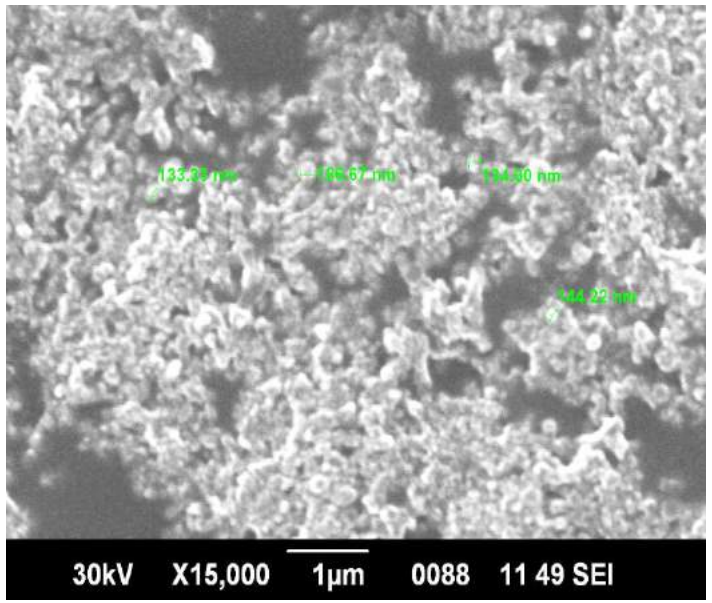


(F)

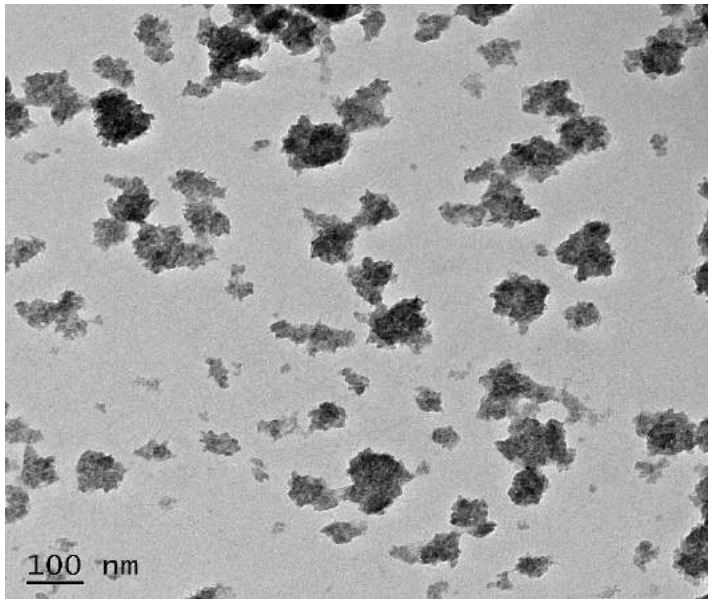

Figure 3

(A)

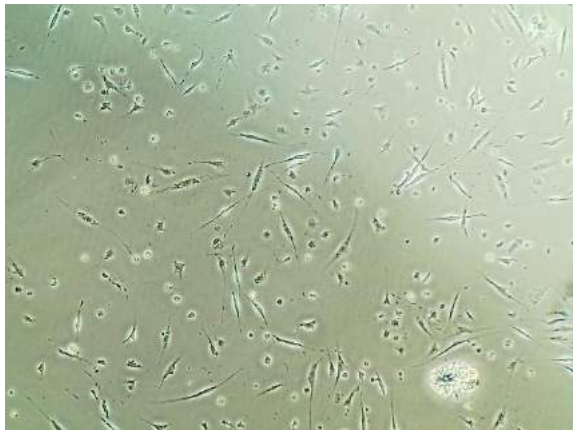

(B)

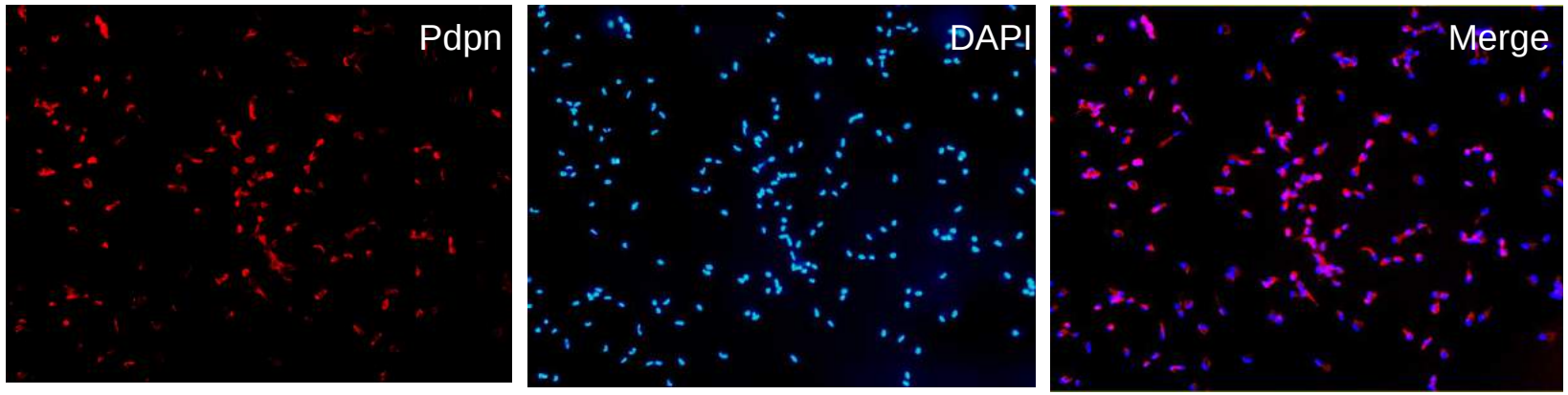

Figure 3

(C)

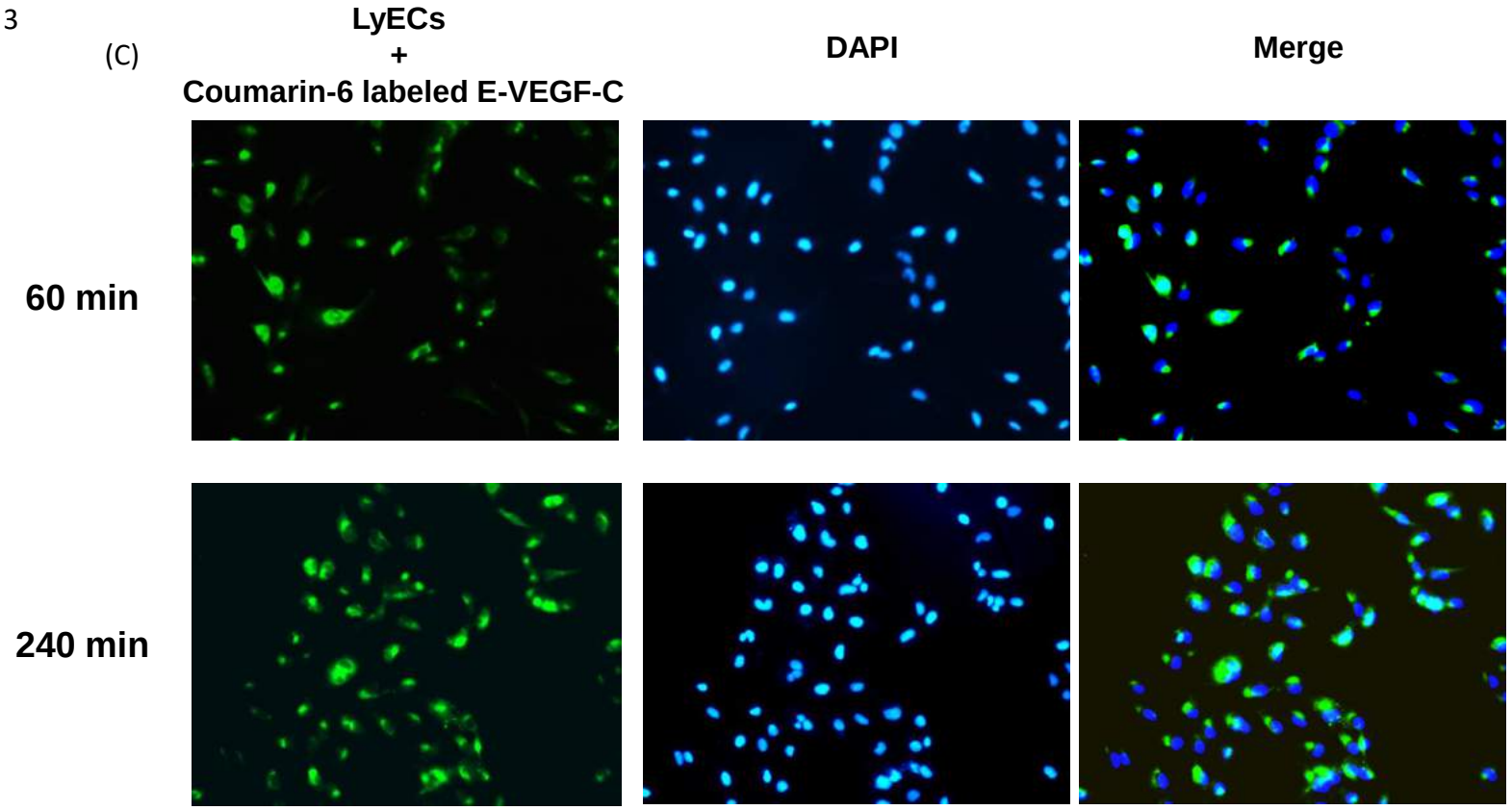
LyECs
+
Coumarin-6 labeled E-VEGF-C
DAPI
Merge
60 min
240 min

(D)

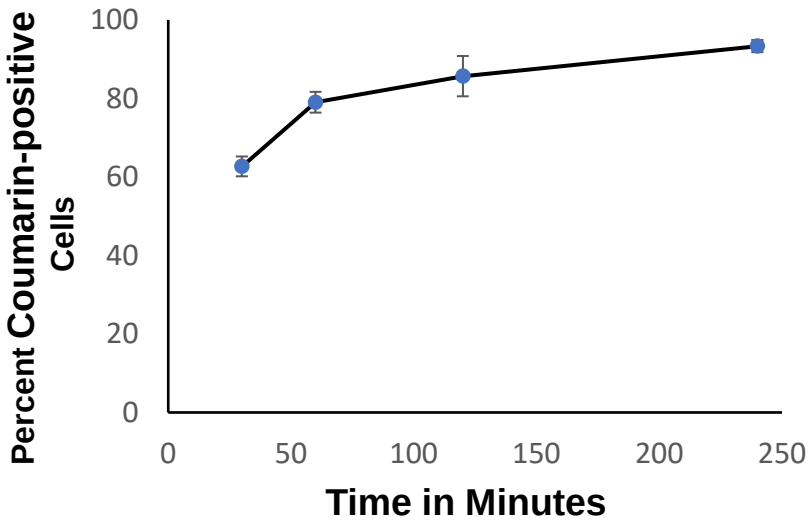
Percent Coumarin-positive Cells
100
80
60
40
20
0
0
50
100
150
200
250
Time in Minutes

Figure 4

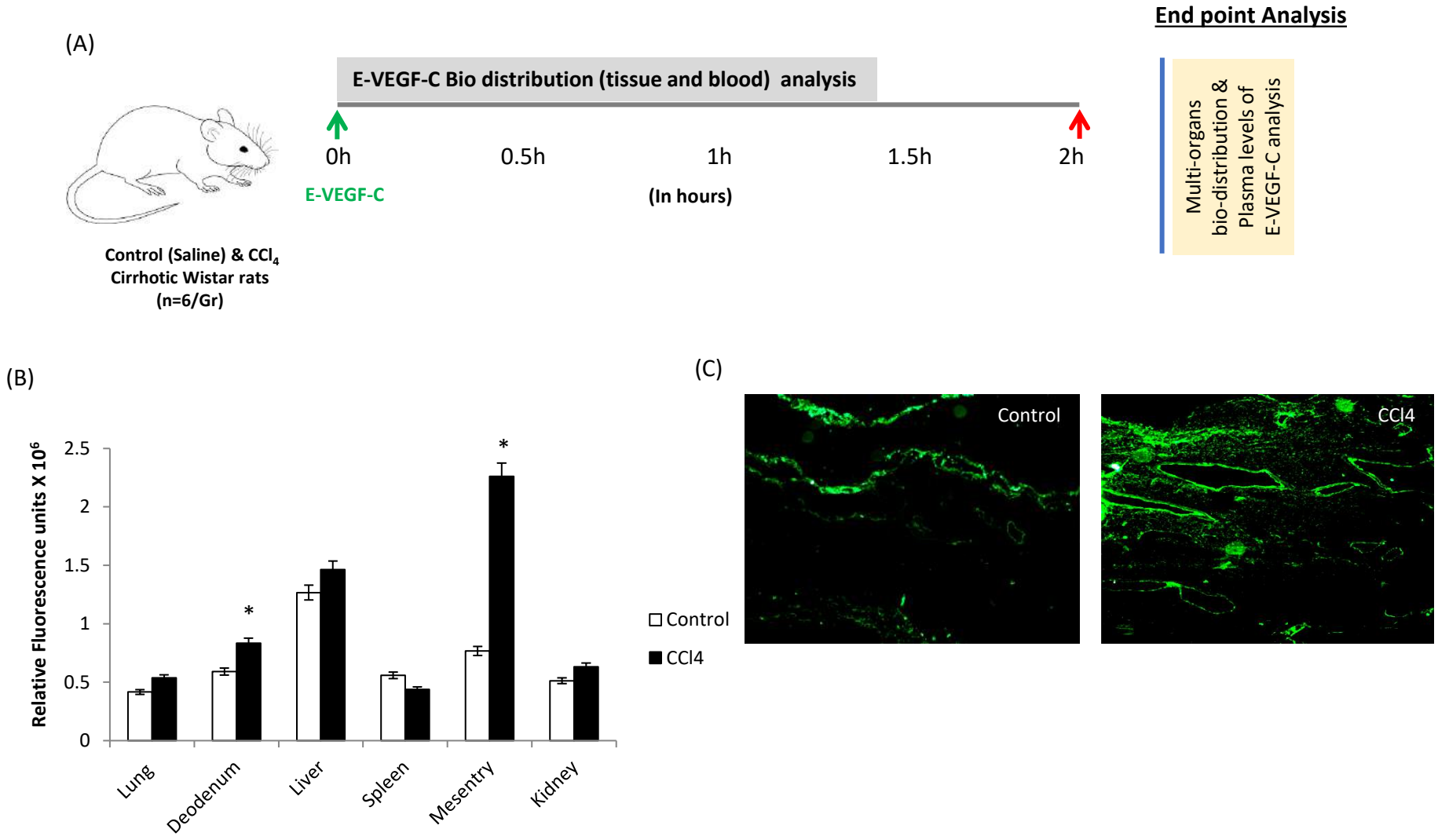
(A)
End point Analysis
E-VEGF-C Bio distribution (tissue and blood) analysis
0h
0.5h
1h
1.5h
2h
E-VEGF-C
(In hours)
Multi-organs bio-distribution & Plasma levels of E-VEGF-C analysis
Control (Saline) & CCl4 Cirrhotic Wistar rats (n=6/Gr)
(B)
Relative Fluorescence units X 10^6
2.5
2
1.5
1
0.5
0
Lung
Deodenum
Liver
Spleen
Mesentry
Kidney
Control
CCl4
(C)
Control
CCl4

Figure 4

(D)

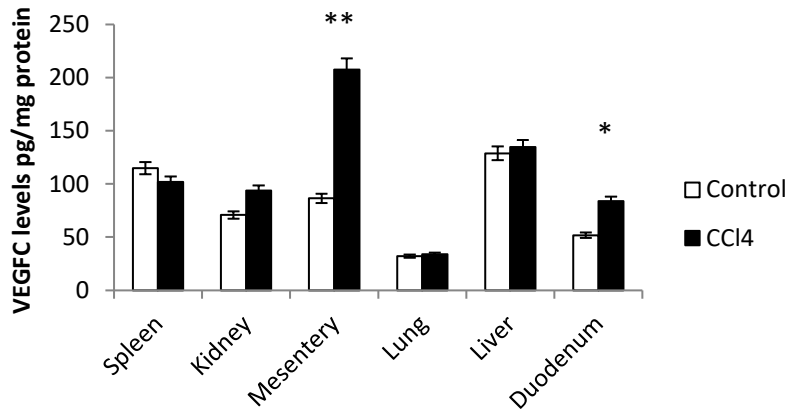
VEGFC levels pg/mg protein
250
200
150
100
50
0
**
*
Control
CCl4
Spleen
Kidney
Mesentery
Lung
Liver
Duodenum

(E)

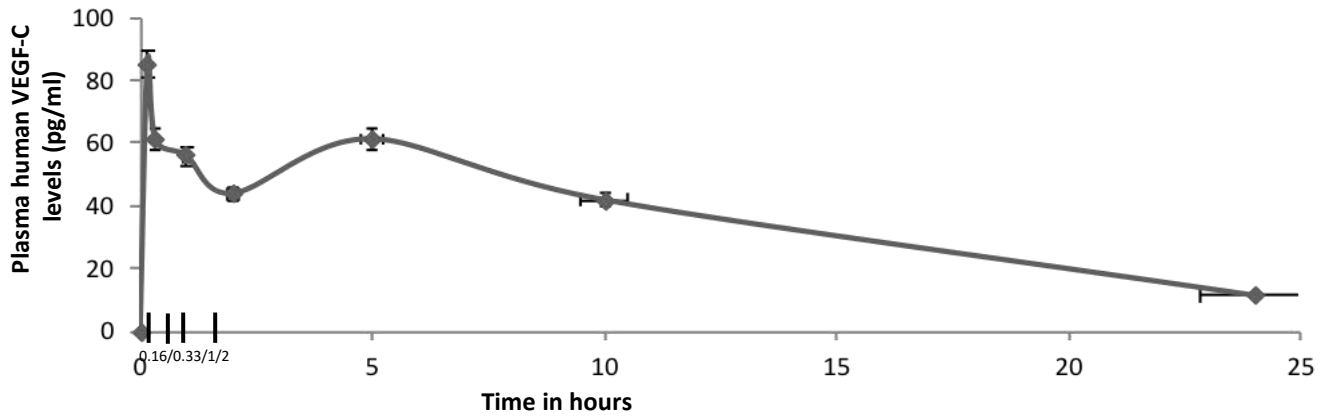
Plasma human VEGF-C levels (pg/ml)
100
80
60
40
20
0
0.16/0.33/1/2
0
5
10
15
20
25
Time in hours

Figure 5

(A)

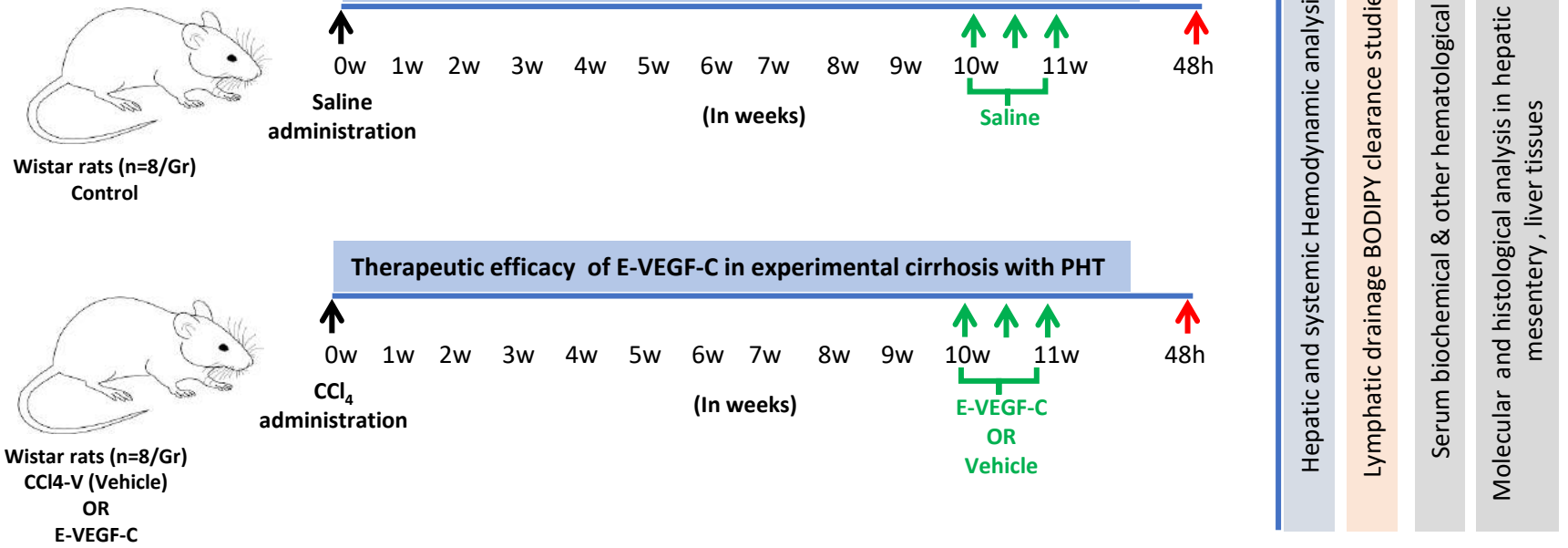
Therapeutic efficacy of E-VEGF-C in experimental cirrhosis with PHT
0w 1w 2w 3w 4w 5w 6w 7w 8w 9w 10w 11w 48h
Saline administration
(In weeks)
Saline
Wistar rats (n=8/Gr)
Control
Therapeutic efficacy of E-VEGF-C in experimental cirrhosis with PHT
0w 1w 2w 3w 4w 5w 6w 7w 8w 9w 10w 11w 48h
CCl4 administration
(In weeks)
E-VEGF-C
OR
Vehicle
Wistar rats (n=8/Gr)
CCl4-V (Vehicle)
OR
E-VEGF-C
Hepatic and systemic Hemodynamic analysis
Lymphatic drainage BODIPY clearance studies
Serum biochemical & other hematological
Molecular and histological analysis in hepatic and mesentery , liver tissues

(B)

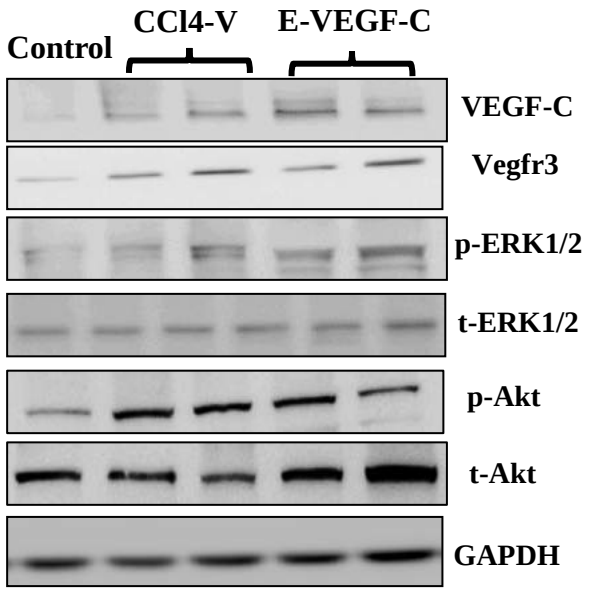
Control
CCl4-V
E-VEGF-C
VEGF-C
Vegfr3
p-ERK1/2
t-ERK1/2
p-Akt
t-Akt
GAPDH

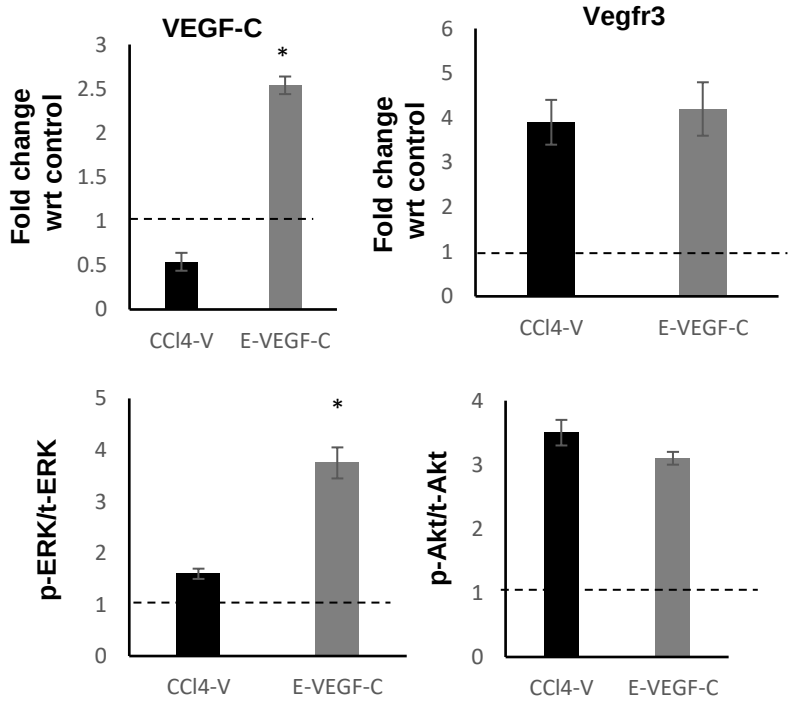
VEGF-C
Fold change wrt control
CCl4-V
E-VEGF-C
Vegfr3
Fold change wrt control
CCl4-V
E-VEGF-C
p-ERK/t-ERK
CCl4-V
E-VEGF-C
p-Akt/t-Akt
CCl4-V
E-VEGF-C

Figure 5

(C)

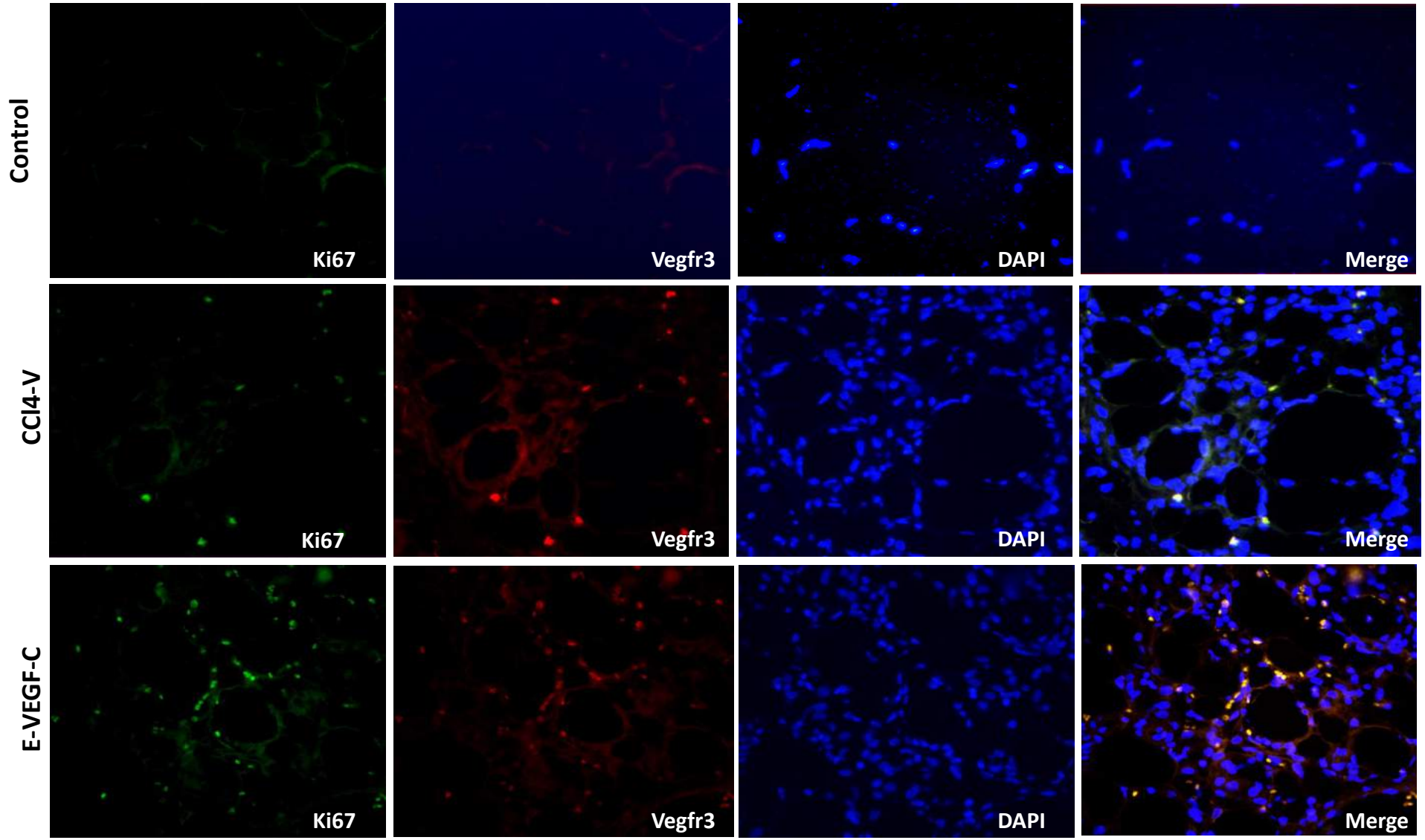
Control
CCl4-V
E-VEGF-C
Ki67
Vegfr3
DAPI
Merge
Ki67
Vegfr3
DAPI
Merge
Ki67
Vegfr3
DAPI
Merge

Figure 5

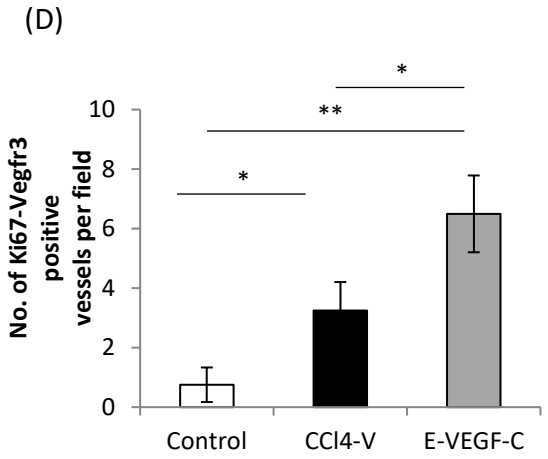
(D)
No. of Ki67-Vegfr3 positive vessels per field
10
8
6
4
2
0
*
**
*
Control
CCl4-V
E-VEGF-C

Figure 5

(E)

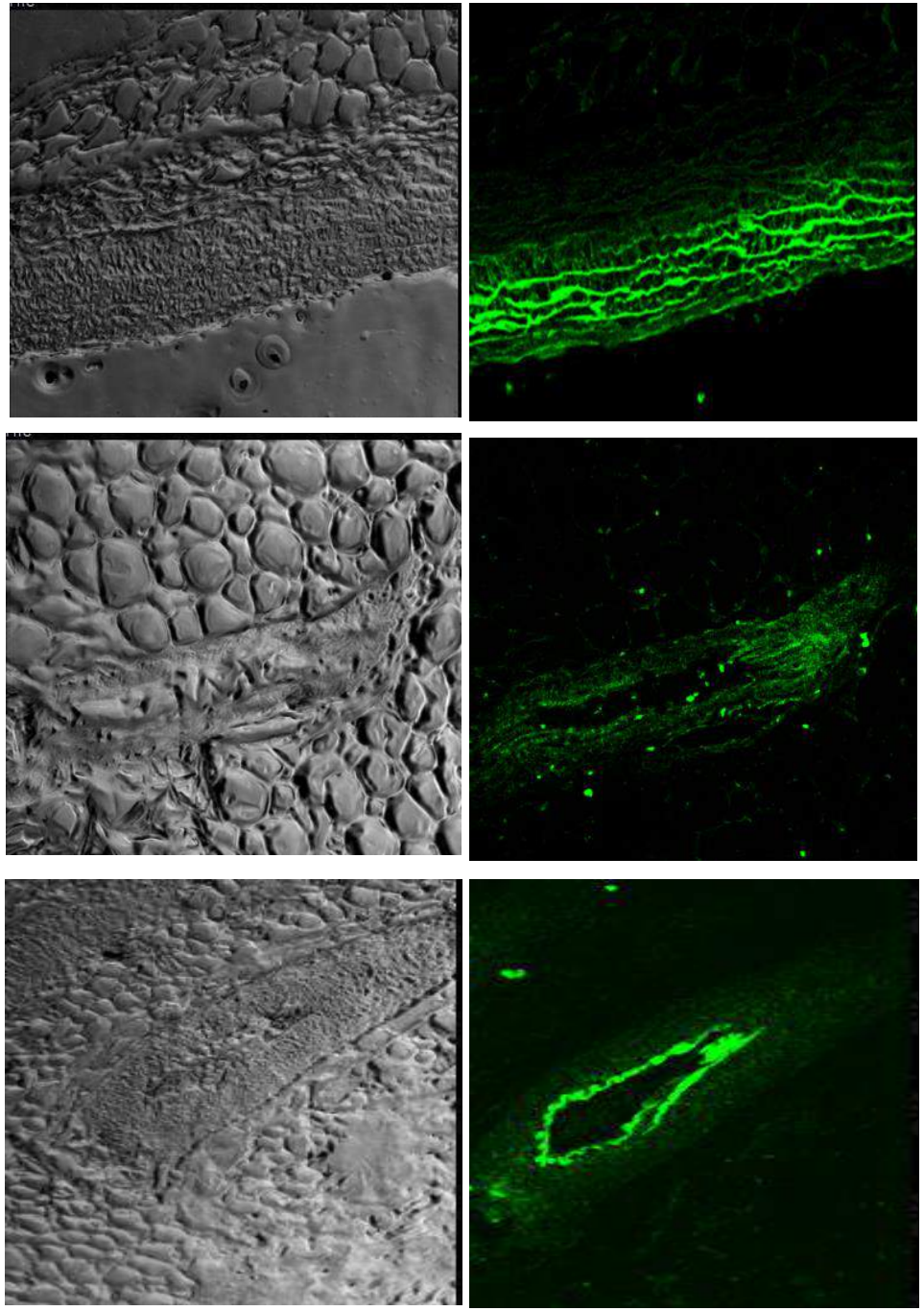

(F)

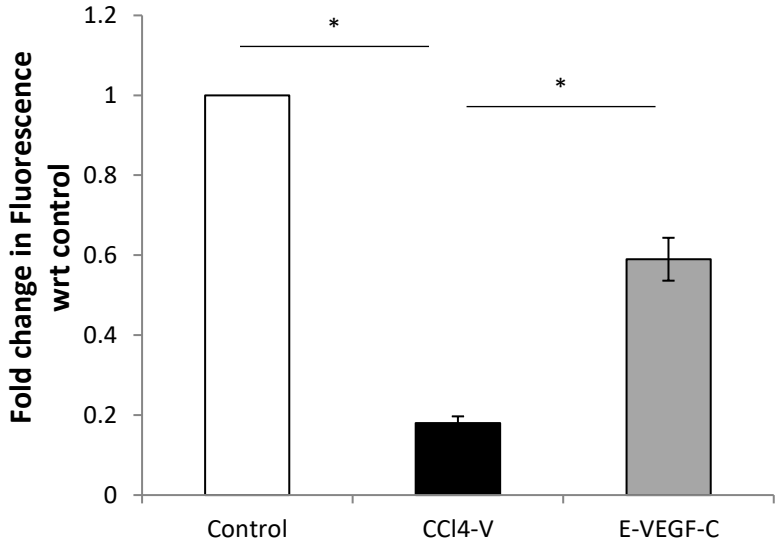
Fold change in Fluorescence wrt control
1.2
1
0.8
0.6
0.4
0.2
0
*
*
Control
CCl4-V
E-VEGF-C

Figure 6

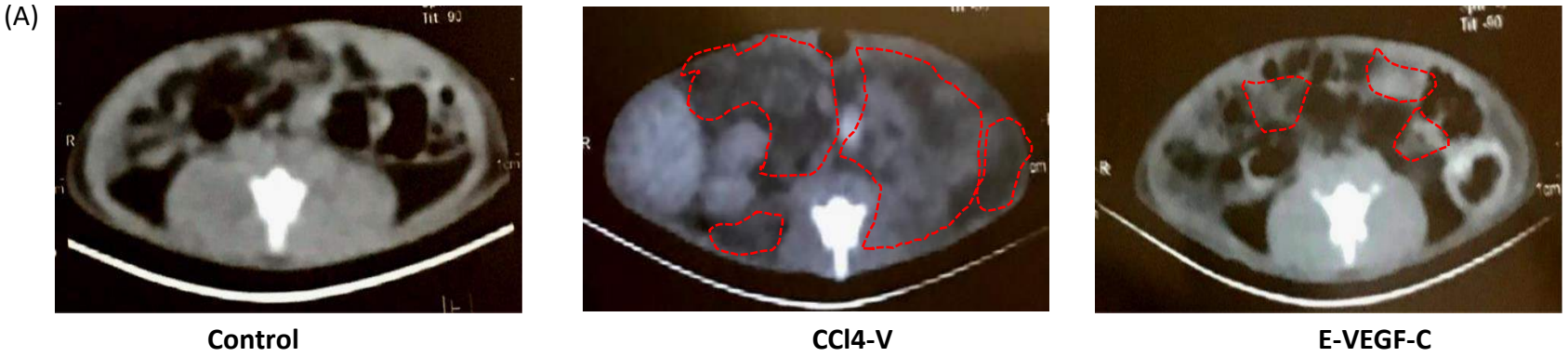
(A)
Control
CCl4-V
E-VEGF-C

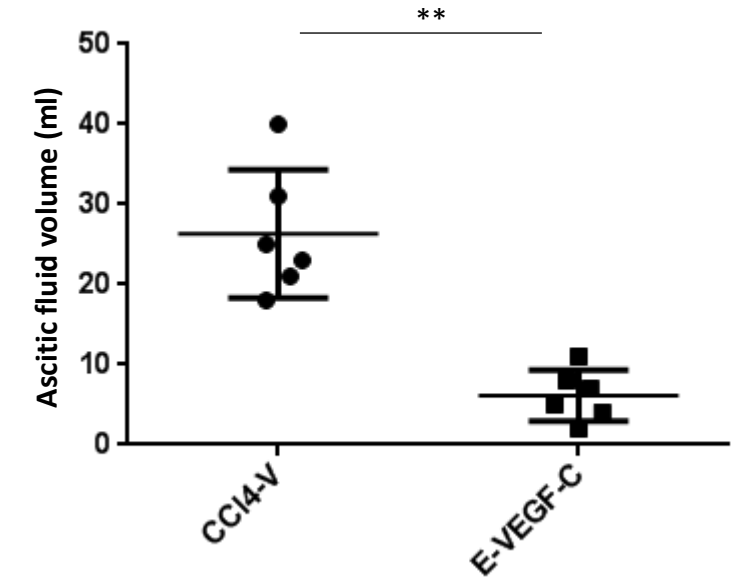
(B)
**
Ascitic fluid volume (ml)
50
40
30
20
10
0
CCl4-V
E-VEGF-C

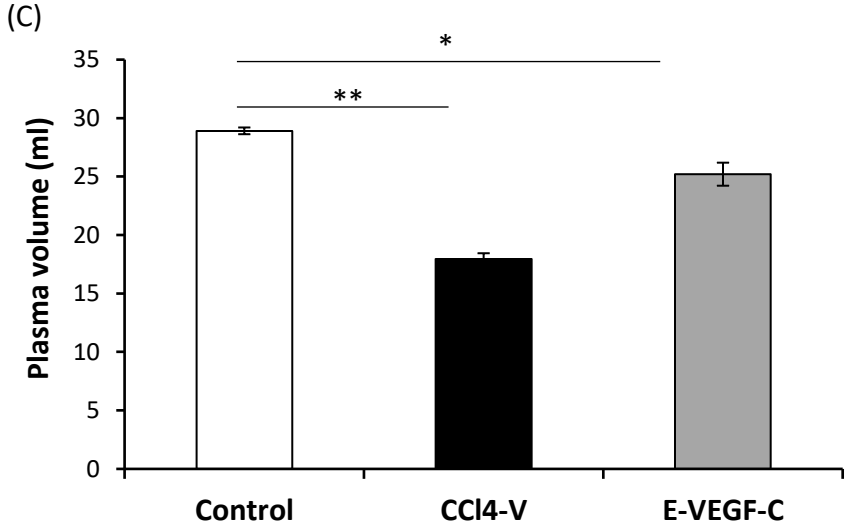
(C)
*
**
Plasma volume (ml)
35
30
25
20
15
10
5
0
Control
CCl4-V
E-VEGF-C

Figure 6

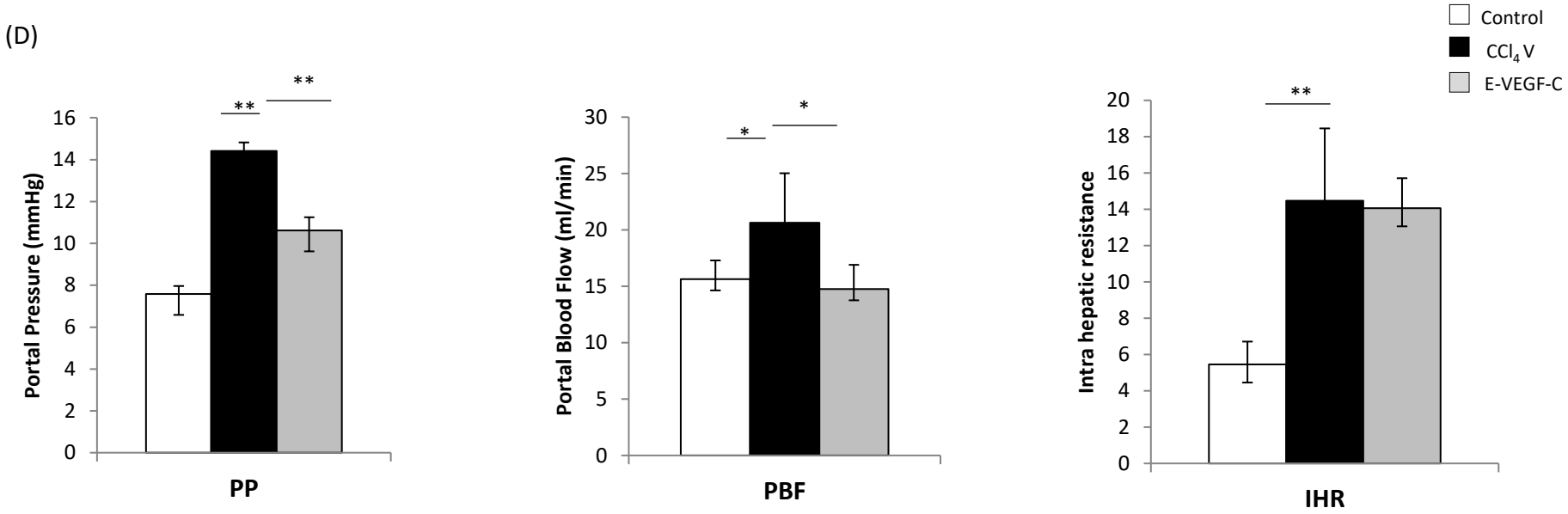
(D)
Control
CCl4 V
E-VEGF-C
Portal Pressure (mmHg)
PP
Portal Blood Flow (ml/min)
PBF
Intra hepatic resistance
IHR
(E)
Control
CCl4-V
E-VEGF-C
No fibrosis
Cirrhosis
Cirrhosis

Figure 6

(F)

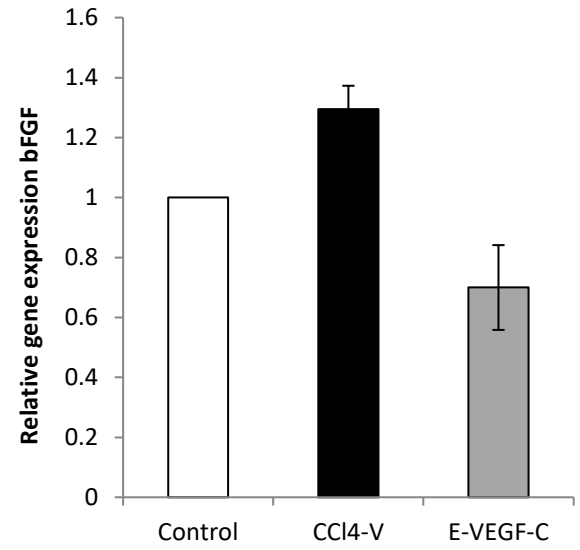
Relative gene expression bFGF
1.6
1.4
1.2
1
0.8
0.6
0.4
0.2
0
Control
CCl4-V
E-VEGF-C

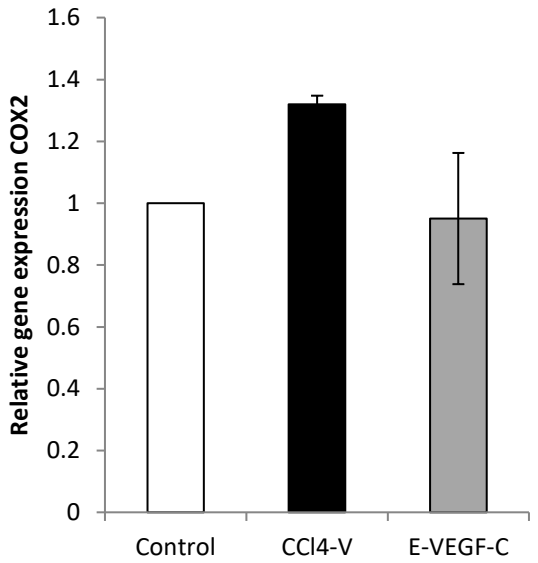
Relative gene expression COX2
1.6
1.4
1.2
1
0.8
0.6
0.4
0.2
0
Control
CCl4-V
E-VEGF-C

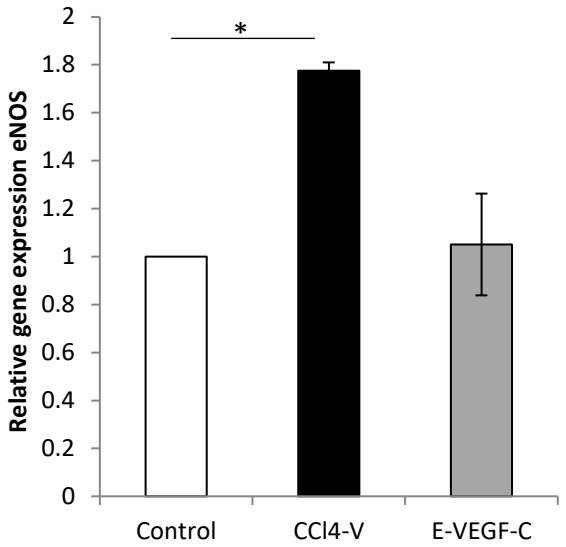
Relative gene expression eNOS
2
1.8
1.6
1.4
1.2
1
0.8
0.6
0.4
0.2
0
*
Control
CCl4-V
E-VEGF-C

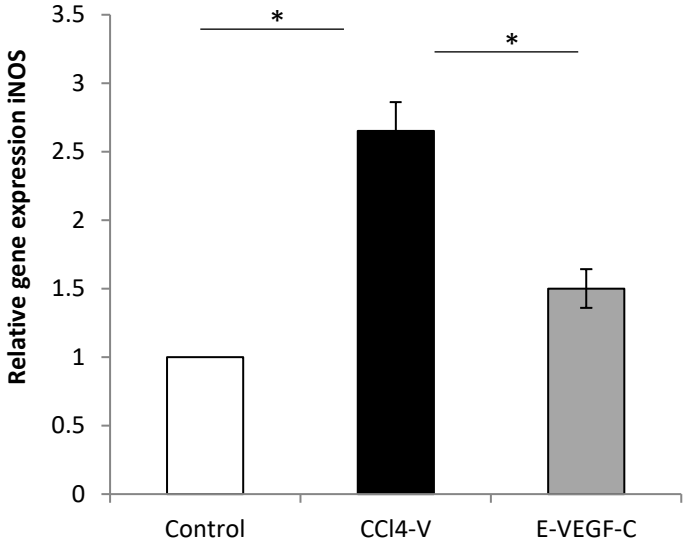
Relative gene expression iNOS
3.5
3
2.5
2
1.5
1
0.5
0
*
*
Control
CCl4-V
E-VEGF-C

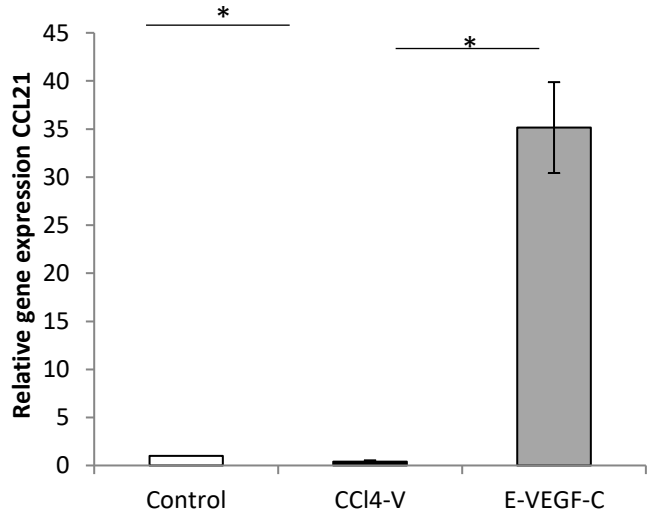
Relative gene expression CCL21
45
40
35
30
25
20
15
10
5
0
*
*
Control
CCl4-V
E-VEGF-C

Figure 6

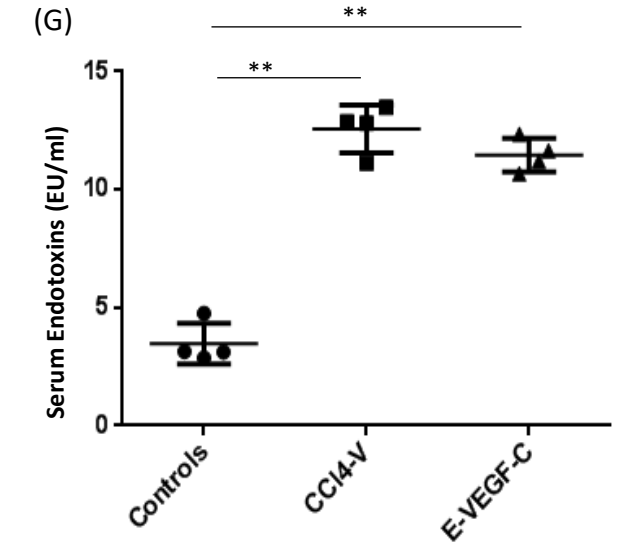
(G)
**
**
Serum Endotoxins (EU/ml)
15
10
5
0
Controls
CCl4-V
E-VEGF-C

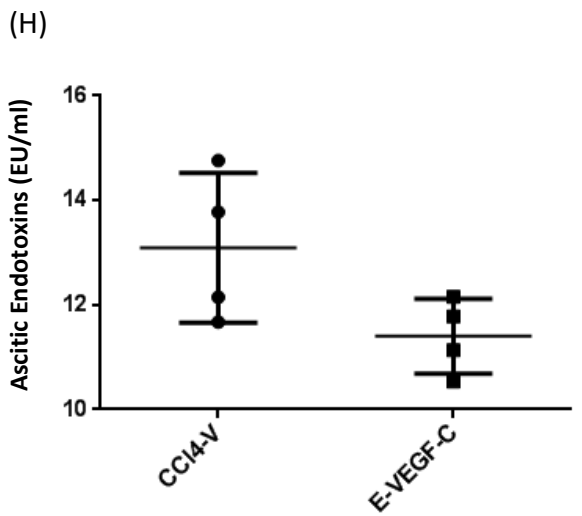
(H)
Ascitic Endotoxins (EU/ml)
16
14
12
10
CCl4-V
E-VEGF-C

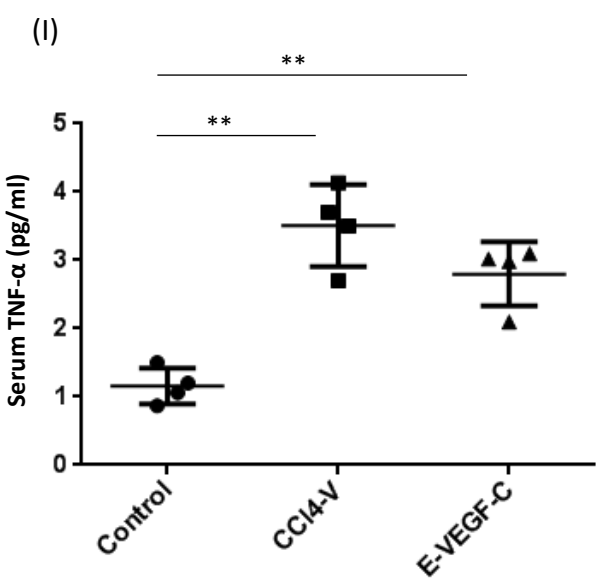
(I)
**
**
Serum TNF-α (pg/ml)
5
4
3
2
1
0
Control
CCl4-V
E-VEGF-C

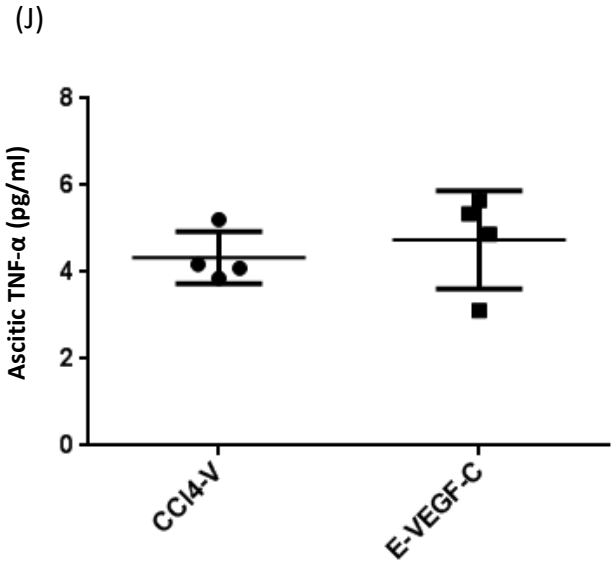
(J)
Ascitic TNF-α (pg/ml)
8
6
4
2
0
CCl4-V
E-VEGF-C

Figure 7

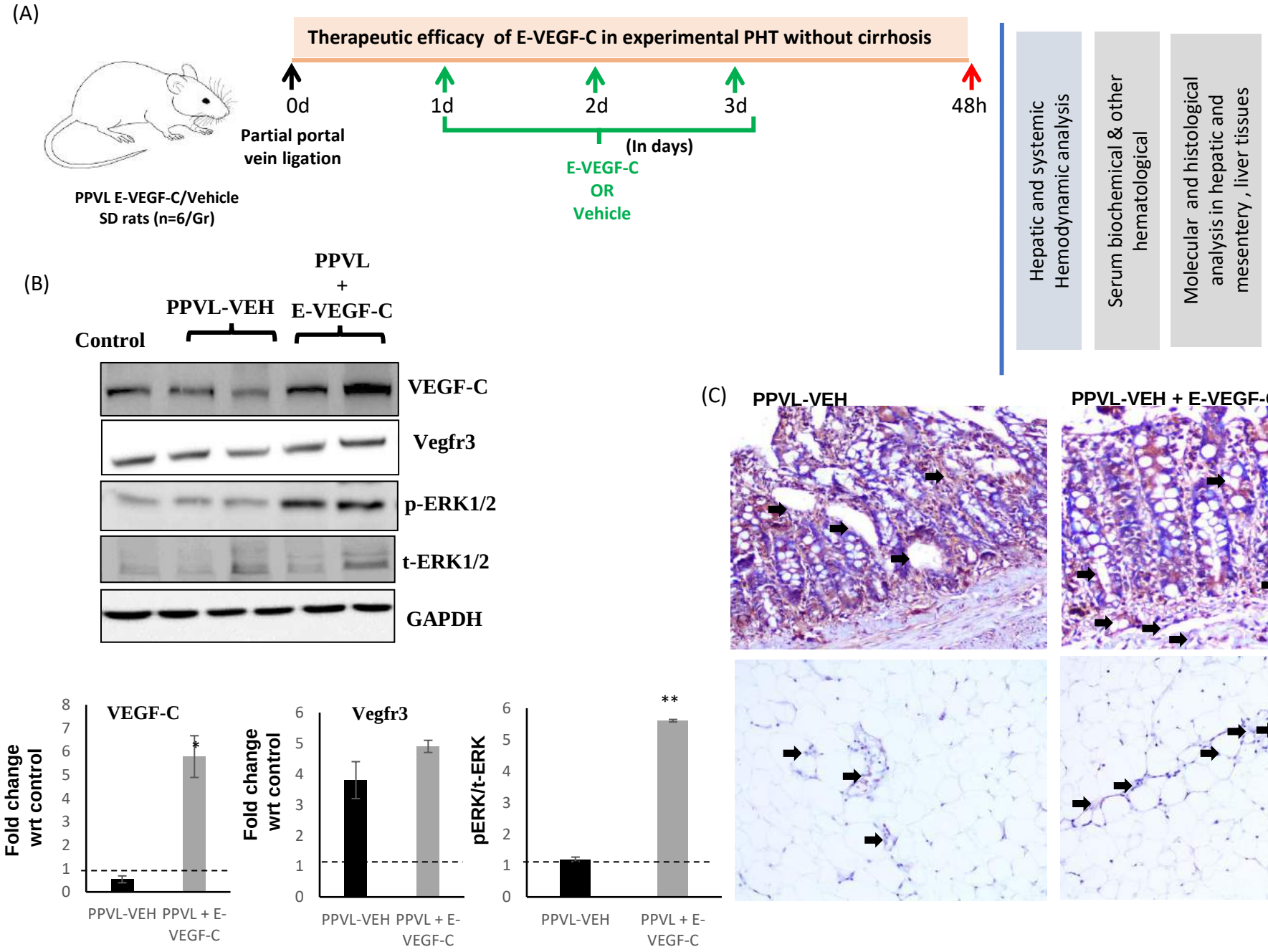
(A)
Therapeutic efficacy of E-VEGF-C in experimental PHT without cirrhosis
0d
1d
2d
3d
48h
Partial portal vein ligation
(In days)
E-VEGF-C OR Vehicle
PPVL E-VEGF-C/Vehicle SD rats (n=6/Gr)
Hepatic and systemic Hemodynamic analysis
Serum biochemical & other hematological
Molecular and histological analysis in hepatic and mesentery , liver tissues
(B)
Control
PPVL-VEH
PPVL + E-VEGF-C
VEGF-C
Vegfr3
p-ERK1/2
t-ERK1/2
GAPDH
Fold change wrt control
VEGF-C
Vegfr3
pERK/t-ERK
PPVL-VEH
PPVL + E-VEGF-C
(C)
PPVL-VEH
PPVL-VEH + E-VEGF-C

Figure 7

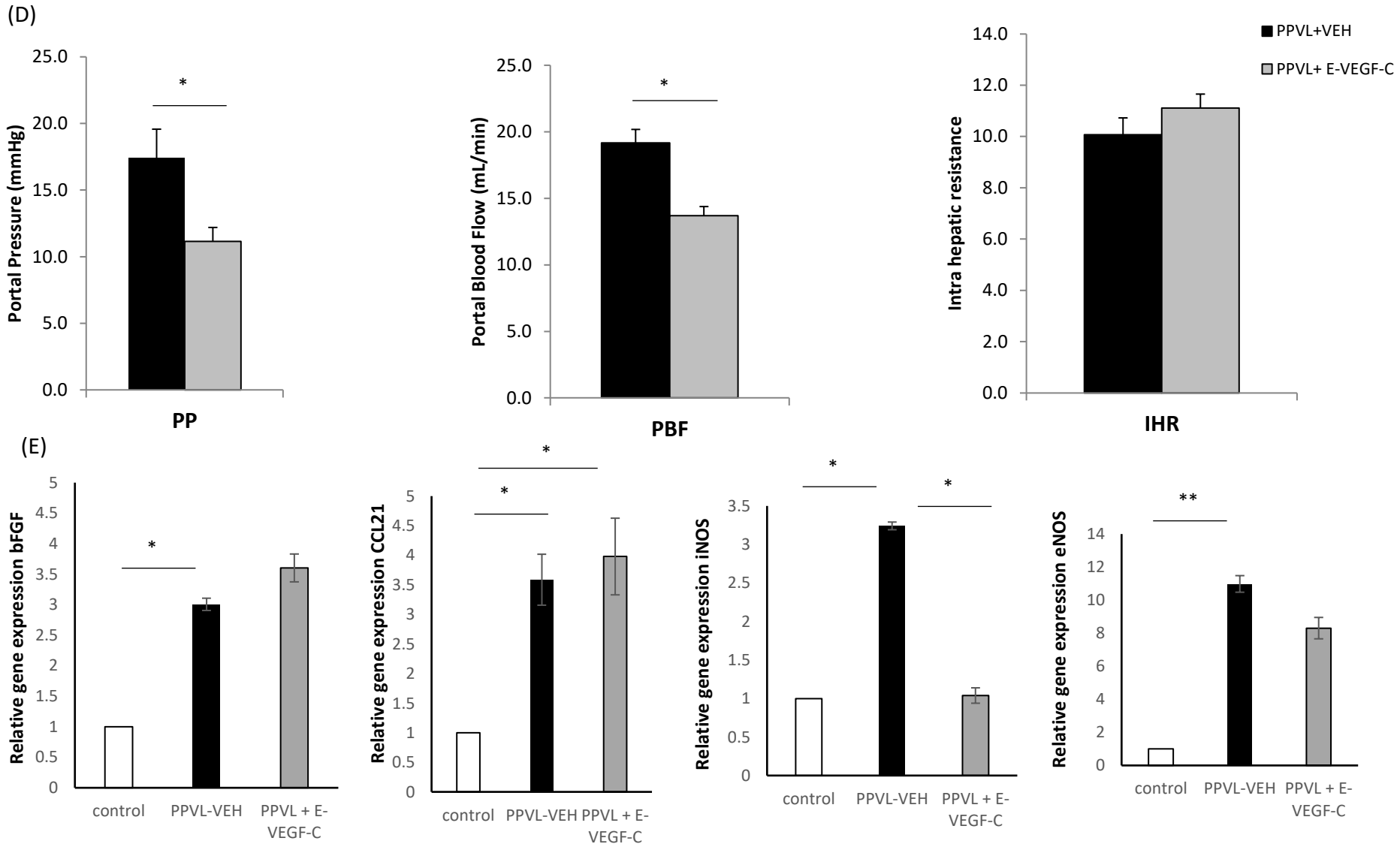
(D)
Portal Pressure (mmHg)
PP
Portal Blood Flow (mL/min)
PBF
Intra hepatic resistance
IHR
PPVL+VEH
PPVL+ E-VEGF-C
(E)
Relative gene expression bFGF
Relative gene expression CCL21
Relative gene expression iNOS
Relative gene expression eNOS
control
PPVL-VEH
PPVL + E-VEGF-C

Figure 8

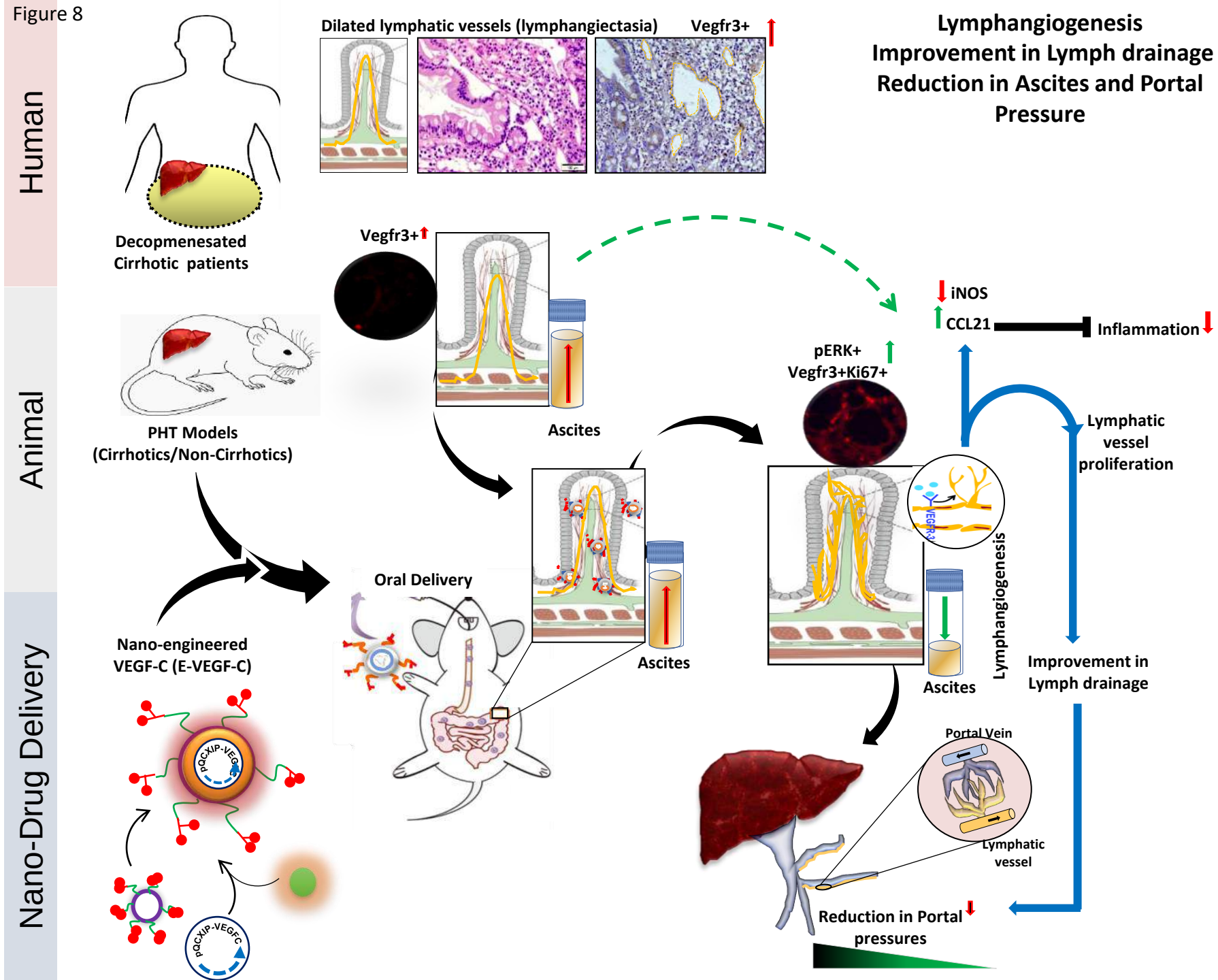
Human
Animal
Nano-Drug Delivery
Gut Lymphatic restoration
Dilated lymphatic vessels (lymphangiectasia)
Vegfr3+
Lymphangiogenesis
Improvement in Lymph drainage
Reduction in Ascites and Portal Pressure
Decopmenesated Cirrhotic patients
PHT Models (Cirrhotics/Non-Cirrhotics)
Nano-engineered VEGF-C (E-VEGF-C)
pQCXIP-VEGFC
Oral Delivery
Ascites
pERK+
Vegfr3+Ki67+
iNOS
CCL21
Inflammation
Lymphatic vessel proliferation
Lymphangiogenesis
Improvement in Lymph drainage
Portal Vein
Lymphatic vessel
Reduction in Portal pressures